



HAL
open science

Distinguishing the roles of thylakoid respiratory terminal oxidases in the cyanobacterium *Synechocystis* sp. PCC 6803

Maria Ermakova, Tuomas Huokko, Pierre Richaud, Luca Bersanini, Christopher Howe, David Lea-Smith, G. Peltier, Yagut Allahverdiyeva

► To cite this version:

Maria Ermakova, Tuomas Huokko, Pierre Richaud, Luca Bersanini, Christopher Howe, et al.. Distinguishing the roles of thylakoid respiratory terminal oxidases in the cyanobacterium *Synechocystis* sp. PCC 6803. *Plant Physiology*, 2016, 171, pp.1307-1319. 10.1104/pp.16.00479 . cea-02484759

HAL Id: cea-02484759

<https://cea.hal.science/cea-02484759>

Submitted on 10 Jan 2024

HAL is a multi-disciplinary open access archive for the deposit and dissemination of scientific research documents, whether they are published or not. The documents may come from teaching and research institutions in France or abroad, or from public or private research centers.

L'archive ouverte pluridisciplinaire **HAL**, est destinée au dépôt et à la diffusion de documents scientifiques de niveau recherche, publiés ou non, émanant des établissements d'enseignement et de recherche français ou étrangers, des laboratoires publics ou privés.

1 **Short title:** The function of terminal oxidases in cyanobacteria

2

3 **Corresponding author details**

4 Yagut Allahverdiyeva

5 Laboratory of Molecular Plant Biology, Department of Biochemistry, University of Turku,
6 Turku, FI-20014, Finland

7 allahve@utu.fi

8

9 **Research area: Primary:** Membranes, transport and biogenetics

10 **Secondary:** Biochemistry and metabolism

11

12

13

14

15

16

17

18

19

20

21

22

23

24

25

26

27

28

29 **Distinguishing the roles of thylakoid respiratory terminal oxidases in the**
30 **cyanobacterium *Synechocystis* sp. PCC 6803¹**

31

32 Maria Ermakova*, Tuomas Huokko*, Pierre Richaud, Luca Bersanini, Christopher J.
33 Howe, David J. Lea-Smith, Gilles Peltier, Yagut Allahverdiyeva[#]

34

35 Laboratory of Molecular Plant Biology, Department of Biochemistry, University of Turku,
36 Turku, FI-20014, Finland (M.E., T.H., L.B., Y.A.);

37 Commissariat à l’Energie Atomique et aux Energies Alternatives, Institut de Biologie
38 Environnementale et de Biotechnologie, Laboratoire de Bioénergétique et Biotechnologie
39 des Bactéries et Microalgues, Cadarache, Saint-Paul-lez-Durance, F-13108, France (P.R.,
40 G.P.);

41 Centre National de la Recherche Scientifique, Biologie Végétale et Microbiologie
42 Environnementales, Unité Mixte de Recherche 7265, F-13108 Saint-Paul-lez-Durance,
43 France (P.R., G.P.);

44 Aix Marseille Université, Biologie Végétale et Microbiologie Environnementales, Unité
45 Mixte de Recherche 7265, Marseille, F-13284, France (P.R., G.P.);

46 Department of Biochemistry, University of Cambridge, UK (D.J.L-S., C.J.H).

47

48 * these authors contributed equally to this work

49

50 **One-sentence summary:** Electron sinks, comprising the O₂ utilizing respiratory terminal
51 oxidases and flavodiiron proteins, contribute to photoprotection and regulation of
52 photosynthesis under light in cyanobacteria.

53

54 **List of author contribution:** Y.A. designed the research, M.E., T.H., P.R., L.B.
55 performed the experiments, analyzed the data; C.J.H. and P.G.P. contributed to the
56 analytical tools; D.J.L-S contributed to the data analysis and analytical tools; M.E., T.H.,
57 D.J.L-S. and Y.A. wrote the article.

58

59 **Funding:** ¹This work was financially supported by the Academy of Finland Finnish Centre
60 of Excellence in Molecular Biology of Primary Producers (2014-2019) project # 271832
61 and by the Kone Foundation (to Y.A.). L.B. was supported by the Alfred Kordelin

62 Foundation, D.J.L-S by the Environmental Services Association Education Trust. Support
63 was also provided by the Héliobiotec platform, funded by the European Union (European
64 Regional Development Fund), the Région Provence Alpes Côte d'Azur, the French
65 Ministry of Research, and the CEA.

66

67 # corresponding author: Yagut Allahverdiyeva, e-mail: allahve@utu.fi

68

69

70

71 **Abstract**

72

73 Various O₂-utilizing electron sinks, including the soluble flavodiiron proteins (Flv1/3), and
74 the membrane-localized respiratory terminal oxidases (RTOs), cytochrome *c* oxidase
75 (Cox) and quinol oxidase (Cyd), are present in the photosynthetic electron transfer chain of
76 *Synechocystis* sp. PCC 6803. However, the role of individual RTOs and their relative
77 importance compared to other electron sinks is poorly understood, particularly under light.
78 Via membrane inlet mass spectrometry gas-exchange, chlorophyll *a* fluorescence, P700
79 analysis and inhibitor treatment of wild-type and various mutants deficient in RTOs,
80 Flv1/3 and photosystem I, we investigated the contribution of these complexes to the
81 alleviation of excess electrons in the photosynthetic chain. For the first time we
82 demonstrated the activity of Cyd in O₂ uptake under light, although it was detected only
83 upon inhibition of electron transfer at the cytochrome *b₆f* site and in $\Delta flv1/3$ under
84 fluctuating light conditions, where linear electron transfer was drastically inhibited due to
85 impaired PS I activity. Cox is mostly responsible for dark respiration and competes with
86 P700 for electrons under high light. Only the $\Delta cox/cyd$ double mutant, but not single
87 mutants, demonstrated a highly reduced PQ pool in darkness and impaired gross O₂
88 evolution under light, indicating that thylakoid-based RTOs are able to compensate
89 partially for each other. Thus both electron sinks contribute to alleviation of excess
90 electrons under illumination: RTOs continue to function under light, operating on slower
91 time ranges and on a limited scale, whereas Flv1/3 responds rapidly as a light-induced
92 component and has greater capacity.

93

94

95

96 Cyanobacteria (oxygenic photosynthetic bacteria) inhabit a range of highly variable
97 aquatic and terrestrial environments, which are diverse in light and in the availability of
98 nutrients. With the exception of *Gloeobacter* species, all cyanobacteria contain a series of
99 internal thylakoid membranes, where a photosynthetic electron transport chain (ETC) is
100 localized. This ETC consists of four major protein complexes: photosystem II (PS II),
101 cytochrome *b₆f* (Cyt *b₆f*), photosystem I (PS I) and ATP synthase, similar to that of
102 eukaryotic photosynthetic organisms (Fig. 1). The photosynthetic electron transfer chain
103 provides energy (ATP) and reducing equivalents (reduced ferredoxin (Fd), NADPH) for
104 carbon anabolism and other vital processes.

105

106 Following absorption of photons by the large external light-harvesting antenna, the
107 phycobilisome, the excitation energy is directed to the reaction centers of PS II and PS I,
108 where charge separation occurs. In PS II, this process is followed by splitting of water to
109 molecular oxygen and protons, which are released into the lumen, and extraction of
110 electrons for the reduction of P680⁺. Electrons ejected from P680, the primary donor of PS
111 II, are forwarded to pheophytin, then to plastoquinone molecules (PQ), Q_A and Q_B.
112 Following double reduction and protonation, plastoquinol (PQH₂) diffuses from the Q_B
113 pocket into the membrane. PQH₂ is oxidized by Cyt *b₆f*, resulting in proton translocation to
114 the lumen and electron transfer to the lumen-localized soluble electron carriers,
115 plastocyanin (Pc) or cytochrome *c₆* (Cyt *c₆*). These small proteins donate electrons to
116 P700⁺, the oxidized primary electron donor of PS I. Electrons extracted from P700 during
117 charge separation are transferred via a chain of cofactors incorporated in PS I to Fd, a
118 soluble electron carrier on the cytosolic side of the thylakoid membrane. The Fd:NADP⁺
119 oxidoreductase (FNR) concludes the linear electron transport chain by catalyzing the
120 formation of NADPH. A proton gradient established during photosynthetic electron
121 transfer is used by ATP synthase for the production of ATP.

122

123 In the model cyanobacterium *Synechocystis* sp. PCC 6803 (hereafter *Synechocystis*) the
124 thylakoid membrane is not just the site of photosynthesis but also respiration (reviewed in
125 Vermaas, 2001; Mullineaux, 2014a; Lea-Smith et al., 2016). The respiratory electron
126 transfer chain transfers electrons extracted from organic molecules into the PQ pool.
127 NAD(P)H dehydrogenase-like complex type 1 (NDH-1), succinate dehydrogenase (SDH)
128 and possibly one to three different NAD(P)H dehydrogenases type 2 (NDH-2) may
129 participate in PQ pool reduction (Mi et al., 1992; Ohkawa et al., 2000; Cooley et al., 2000;

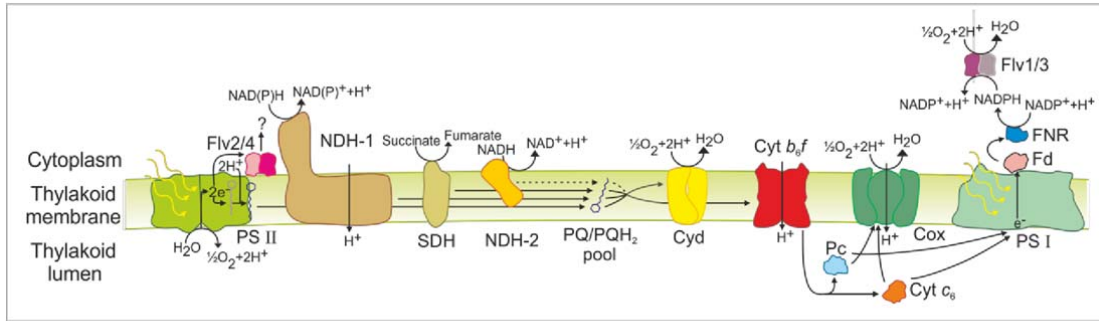


Figure 1. Schematic diagram of the thylakoid membrane-localized photosynthetic and respiratory electron transfer chains. Lines indicate electron transport; dotted lines indicate possible but poorly characterized electron transfer pathways. PS II, Photosystem II; Flv2/4, Flavodiiron proteins 2/4; Flv1/3, Flavodiiron proteins 1/3; PQ, plastoquinone; PQH₂, plastoquinol; Cyt *b₆f*, cytochrome *b₆f* complex; Pc, plastocyanin; Cyt *c₆*, cytochrome *c₆*; PS I, Photosystem I; Fd, ferredoxin; FNR, ferredoxin-NADP⁺ oxidoreductase; NDH-1, NAD(P)H dehydrogenase-like complex type 1; SDH, succinate dehydrogenase; NDH-2, NAD(P)H dehydrogenase type 2; Cyt *bd* quinol oxidase; Cox, cytochrome *c* oxidase.

130 Howitt et al., 1999). PQH₂ oxidation can then occur via either Cyt *b₆f* or respiratory
 131 terminal oxidases (RTOs). In *Synechocystis*, the cytochrome *bd* quinol oxidase (Cyt),
 132 encoded by *cydAB*, reduces O₂ with electrons presumably taken directly from the PQ pool
 133 (Berry et al., 2002). Although Cyt does not pump protons across the membrane, it
 134 contributes to the thylakoid membrane potential by releasing protons from PQH₂ oxidation
 135 into the lumen, and by generating water using protons removed from the cytoplasm
 136 (reviewed in Hart et al., 2005). The *aa₃*-type cytochrome *c* oxidase complex (Cox),
 137 encoded by *coxBAC*, is situated only in the thylakoid membrane and can accept electrons
 138 from Pc and Cyt *c₆* (Howitt and Vermaas, 1998; Nomura et al., 2006; Lea-Smith et al.,
 139 2013). Therefore, Cyt *b₆f*, the PQ pool and Pc/Cyt *c₆* are shared by both the photosynthetic
 140 and respiratory electron transfer chains (Scherer, 1990). Cox is present in all cyanobacteria
 141 sequenced thus far (Pils and Shmetterer, 2001; Lea-Smith et al., 2013). Based on similarity
 142 with better characterized *aa₃*-type cytochrome *c* oxidase complexes from other bacteria,
 143 Cox can potentially couple the transfer of electrons to O₂ with the translocation of protons
 144 across the membrane (Iwata et al., 1995; Brändén et al., 2006).

145

146 An additional electron transport chain is localized in the cytoplasmic membrane, which
 147 lacks Cox (Huang et al., 2002) and Cyt *b₆f* (Schultze et al., 2009). This simpler pathway
 148 consists of electrons donated to PQ by NDH-2 and/or SDH, followed by transfer from

149 PQH₂ to RTOs. Localization of Cyd in the thylakoid membrane has been confirmed but
150 this complex may also be present in the cytoplasmic membrane (Howitt and Vermaas,
151 1998; Berry et al., 2002). Another RTO, the alternative oxidase complex (ARTO), encoded
152 by *ctaCIIDIIEII*, probably oxidizes the PQ pool and has been localized only to the
153 cytoplasmic membrane in *Synechocystis* (Huang et al., 2002; Pisareva et al., 2007). Thus
154 ARTO does not have a significant impact on photosynthetic electron transfer (Abramson et
155 al., 2000; Lea-Smith et al., 2013). However, a recent study suggested a possible role for
156 ARTO in reductive Fe uptake (Kranzler et al., 2014). An additional quinol oxidase, which
157 is closely related to the plastid terminal oxidase (PTOX) of plants, has been identified in a
158 range of cyanobacteria but is not present in *Synechocystis* (McDonald et al., 2011).

159

160 The main role of RTOs is to provide metabolic energy required during dark periods
161 (Matthijs and Lubberding, 1988). RTOs are not essential in *Synechocystis* when cells are
162 subjected to continuous moderate or high light (Lea-Smith et al., 2013, Howitt and
163 Vermaas, 1998; Pils and Schmetterer, 2001), or 12 h dark/12 h moderate light (40 μmol
164 photons m⁻² s⁻¹) cycle regimes (Lea-Smith et al., 2013). However, the presence of Cox is
165 essential for viability under low light (Kufryk and Vermaas, 2006) and the presence of at
166 least one thylakoid-based RTO (Cyd or Cox) is required for survival under a 12 h dark/12
167 h high light (150 μmol photons m⁻² s⁻¹) square cycle regime (Lea-Smith et al., 2013).

168

169 Studies of RTO mutants by gas-exchange under light are complicated in oxygenic
170 photosynthetic organisms, due to the O₂ evolving activity of PS II and the existence of
171 other processes capable of O₂ photoreduction. Flavodiiron proteins Flv1 and Flv3 are
172 responsible for the majority of O₂ uptake in the light in cyanobacteria (Allahverdiyeva et
173 al., 2011; Helman et al., 2003, 2005). These proteins likely form a functional couple
174 (Flv1/3) and reduce O₂ directly to water, conceivably, using NADPH formed as a result of
175 linear electron transfer (Vicente et al., 2002; Helman et al., 2003). Moreover,
176 cyanobacteria possess an active photorespiratory metabolism (Eisenhut et al., 2006, 2008)
177 and photorespiratory O₂ uptake plausibly contributes to the total O₂ uptake in the light and
178 in particular during C_i limitation (Allahverdiyeva et al., 2011). Therefore, the role of
179 individual RTOs and their relative importance compared to other electron sinks under light
180 conditions is poorly studied. In this work we used wild-type (WT) and various mutants of
181 *Synechocystis* in combination with specific inhibitors targeting electron transfer chain
182 components, to address the role of RTOs in the light. We demonstrate that Cyd is the key

183 RTO under light, capable of light-induced O₂ uptake under sub-optimal conditions. By
184 contrast, Cox is responsible for the majority of dark respiration but can also contribute to
185 regulation of electron flow to PS I under light in specific cases.

186

187

188 **RESULTS**

189 **Light-induced O₂ uptake in *Synechocystis* cells in the absence and presence of**
190 **inhibitors.**

191 For a precise study of O₂ uptake in *Synechocystis* cells we used Membrane Inlet Mass
192 Spectrometry (MIMS) and ¹⁸O₂-enriched O₂. In contrast to a classical oxygen electrode,
193 which only measures net O₂ production under illumination, MIMS analysis can
194 differentiate between gross O₂ produced by PS II and O₂ uptake under illumination based
195 on increase of ¹⁶O₂ and decrease of ¹⁸O₂, respectively, in the reaction medium. When O₂
196 exchange was monitored in cultures during dark to light (400 μmol photons m⁻² s⁻¹)
197 transition, the WT demonstrated strong O₂ uptake of 34.6±6.7 μmol O₂ [mg Chl]⁻¹ h⁻¹
198 under illumination, which was drastically higher than the O₂ uptake of the cells in darkness
199 (8.3±1.2 μmol O₂ [mg Chl]⁻¹ h⁻¹ (Fig. 2, Fig. S1, the averaged values and SDs are provided
200 in Table 1). The difference between light and dark O₂ uptake rates is defined as the light-
201 induced O₂ uptake rate. The *Δflv1/3* mutant lacking the Flv1 and Flv3 proteins
202 demonstrated a slightly higher O₂ uptake rate in darkness than the WT (10.8±1.6 μmol O₂
203 [mg Chl]⁻¹ h⁻¹), and a similar O₂ uptake rate in the light to that in darkness (Fig. S1). Thus,
204 a strong light-induced O₂ uptake component observed in the WT was missing in the
205 *Δflv1/3*. This was in line with previous reports, demonstrating that O₂ uptake in WT
206 *Synechocystis* was strongly stimulated in the light due to Flv1/3 activity occurring
207 downstream of PS I (Helman et al., 2003, 2005; Allahverdiyeva et al., 2011, 2013, Mustila
208 et al. 2016).

209

210 To investigate a possible role of RTOs functioning at the PQ pool level and to exclude
211 contribution of the Flv1/3 to light-induced O₂ uptake, we performed MIMS experiments in
212 the presence of 2,5-dibromo-6-isopropyl-3-methyl-1,4-benzoquinone (DBMIB), an
213 inhibitor of PQH₂ oxidation at the site of Cyt *b₆f* (Trebst et al., 1970; Yan et al., 2006). In
214 WT cells in the presence of DBMIB, the dark O₂ uptake rate was 10.1±1.5 μmol O₂ [mg
215 Chl]⁻¹ h⁻¹, whereas in the light the rate of total O₂ uptake was two-fold higher than that in
216 darkness (21.1±2.8 μmol O₂ [mg Chl]⁻¹ h⁻¹) (Fig. 2, Table 1). This demonstrates that a
217 strong light-induced O₂ uptake is occurring in WT cells in the presence of DBMIB. To
218 clarify the origin of this O₂ uptake we supplemented the cells, in addition to DBMIB, with
219 2,6 dichloro-*p*-benzoquinone (DCBQ), an artificial acceptor of electrons from PS II (Graan
220 and Ort, 1986). Under these conditions, light-induced O₂ uptake was completely

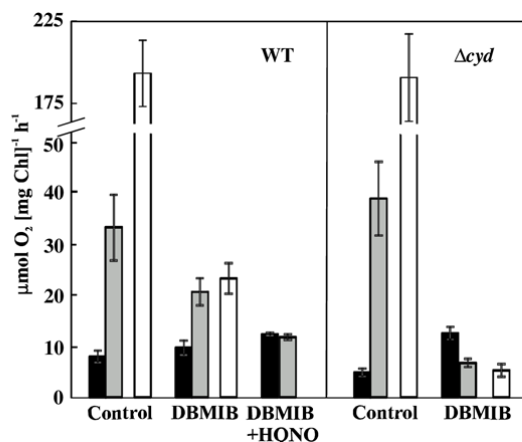


Figure 2. The rates of O₂ exchange in the WT and Δcyd mutant cells incubated in darkness for 5 min and then illuminated with a strong white light (400 $\mu\text{mol photons m}^{-2} \text{s}^{-1}$) for the next 5 min. Black bars and grey bars indicate the rates of total O₂ uptake by cells in darkness and under the light, respectively; white bars indicate the gross O₂ production rate. Measurements were performed either in the absence of inhibitors (control) or in the presence of DBMIB or DBMIB + HQNO. Mean \pm SD, n=3-5.

221 eliminated (Fig. S2A), implying strong competition between DCBQ and an unknown
 222 acceptor which can mediate the light-driven flow of electrons to O₂.

223 Importantly, in the presence of DBMIB, the gross O₂ evolution rate of WT cells decreased
 224 significantly (from $193.3 \pm 20.1 \mu\text{mol O}_2 [\text{mg Chl}]^{-1} \text{h}^{-1}$ in the control cells to 24.2 ± 3.1
 225 $\mu\text{mol O}_2 [\text{mg Chl}]^{-1} \text{h}^{-1}$, Fig. 2, Table 1), becoming nearly equal to the total O₂ uptake rate
 226 under the light. Consequently, the rate of net photosynthesis in the presence of DBMIB
 227 was close to zero (Table 1).

228

229 Next we used 2-n-heptyl-4-hydroxyquinoline N-oxide (HQNO), an inhibitor of Cyd (Pils
 230 et al., 1997). Supplementation of the DBMIB-treated cells with HQNO also completely
 231 eliminated the light-induced component of O₂ uptake (Fig. 2, Table 1). Thus the rate of O₂
 232 uptake was observed to be similar between darkness and light, suggesting that Cyd is
 233 responsible for the light-induced fraction of O₂ uptake under the studied conditions.
 234 Addition of HQNO alone to the WT cells did not significantly affect total O₂ uptake under
 235 light (Fig. S2B), presumably due to the compensatory effect of other O₂ consuming
 236 pathways, such as Cox and Flv1/3.

237

238 It is important to note that the addition of DBMIB also increased dark O₂ uptake in WT
 239 *Synechocystis* cells (from $8.3 \pm 1.2 \mu\text{mol O}_2 [\text{mg Chl}]^{-1} \text{h}^{-1}$ to $10.1 \pm 1.5 \mu\text{mol O}_2 [\text{mg Chl}]^{-1}$
 240 h^{-1} , Table 1), which is in line with a previous report (Zhang et al., 2013). This result raises
 241 a question whether DBMIB itself could act as an electron shuttle to O₂ (Bukhov et al.,

242 2003; Belatik et al., 2013), thus making interpretations difficult. In order to clarify the
243 origin of increased O₂ uptake in the presence of DBMIB, the WT cells were further treated
244 with KCN, which is an inhibitor of both Cyd and Cox (Howitt and Vermaas 1998).
245 Addition of KCN to the DBMIB-treated WT cells completely abolished the light-induced
246 component of O₂ uptake, suggesting a role for RTOs (Fig. S2C). However O₂ uptake in
247 darkness decreased only slightly in the presence of KCN, demonstrating a residual O₂
248 uptake with a rate of about 7.4 μmol O₂ [mg Chl]⁻¹ h⁻¹ occurring similarly under both
249 darkness and light conditions in DBMIB supplemented cells (Fig. S2C). This suggests the
250 existence of “background” O₂ uptake in the presence of DBMIB. Importantly this
251 “background” O₂ uptake is insensitive to light, therefore would not affect the interpretation
252 of light induced O₂ uptake in the WT. To clarify further the effect of this compound, we
253 measured O₂ evolution rates of WT cells supplemented with different DBMIB
254 concentrations using a Clark-type electrode. With increasing DBMIB concentrations the
255 net O₂ production decreased gradually to almost zero at a concentration of 25 μM DBMIB
256 (Fig. S2D), which is in line with the MIMS experiments (Table 1), and suggests that
257 DBMIB act as an electron transfer inhibitor in *Synechocystis* cells. Our results differ from
258 Belatik et al. (2013), which describe high O₂ production rates even at low DBMIB
259 concentrations, and concluded that DBMIB could act as electron acceptor for PS II in
260 spinach thylakoids. This discrepancy could be due to different experimental set ups and the
261 different organisms used.

262

263 **Light-induced O₂ uptake in *Synechocystis* cells deficient in RTOs.**

264 In order to confirm the results obtained with the inhibitors, we subjected mutants deficient
265 in Cyd, Cox and Cox/Cyd to MIMS analysis, first in the absence of inhibitors (Table 1).
266 Dark respiration was reduced in the Δ*cyd* and Δ*cox* mutants and almost abolished in
267 Δ*cox/cyd*. Interestingly, light-induced O₂ uptake was significantly higher in both the Δ*cyd*
268 and Δ*cox* mutants compared to the WT, presumably due to up-regulation of the other RTO
269 pathway (Fig. 2, Table 1). In line with this, Δ*cox/cyd* demonstrated nearly similar light-
270 induced O₂ uptake rates to the WT. Likewise, the total light O₂ uptake was also increased
271 in the single mutants, whereas substantial decrease was observed in Δ*cox/cyd* compared to
272 the WT. All RTO-deficient mutants demonstrated similar gross and net O₂ production rates
273 to WT cells (Table 1).

274

275 In the presence of DBMIB, the rate of dark O₂ uptake was similar between all strains,
276 whereas the light-induced O₂ uptake was completely inhibited in the Δcyd and $\Delta cox/cyd$
277 mutants, and also significantly reduced in Δcox (Table 1). Overall, this resulted in a greatly
278 reduced rate of total O₂ uptake under light in Δcyd and $\Delta cox/cyd$, but not in Δcox . DBMIB
279 also caused a drastic reduction in gross O₂ production in Δcyd and $\Delta cox/cyd$, so that the
280 rates were equal to the total O₂ uptake rates under light, as observed in WT cells. The
281 addition of HQNO to the DBMIB-treated cells did not alter O₂ uptake rates in Δcyd cells.
282 Similar to the WT, the addition of DBMIB and HQNO to Δcox eliminated light-induced
283 O₂ uptake detected in the presence of DBMIB only. These results correlated with the
284 experiments performed on WT cells with inhibitors and confirmed that Cyd is responsible
285 for the majority of light-induced O₂ uptake in the presence of DBMIB.

286

287 **The impact of RTOs under fluctuating light conditions**

288 It was recently reported that the $\Delta flv1/3$ mutant exposed to fluctuating light (FL)
289 conditions exhibited extensive damage to PS I, a drastic decrease in net photosynthesis and
290 to the KCN-sensitive component of light-induced O₂ uptake (Allahverdiyeva et al., 2013).
291 To address a possible role of Cyd in light-induced O₂ uptake under FL conditions, MIMS
292 analysis was undertaken in WT and $\Delta flv1/3$ cells incubated under the FL 20/500 regime
293 (20 $\mu\text{mol photons m}^{-2} \text{s}^{-1}$ background light interrupted by 30 s pulses of 500 $\mu\text{mol photons}$
294 $\text{m}^{-2} \text{s}^{-1}$ light every 5 min) for 3 days. The samples were analyzed either in the absence
295 (control) or in the presence of HQNO, following illumination of the cells with strong white
296 light of 400 $\mu\text{mol photons m}^{-2} \text{s}^{-1}$. In WT cells, the addition of HQNO did not significantly
297 affect the light-induced fraction of O₂ uptake (Fig. 3). Interestingly, the addition of HQNO
298 to $\Delta flv1/3$ cells acclimated to FL conditions resulted in an 86% inhibition of the light-
299 induced O₂ uptake rate, indicating a significant contribution of Cyd to O₂ uptake in the
300 light.

301

302 To investigate further a possible role for Cyd and Cox in the acclimation of cyanobacterial
303 cells to fluctuating light, the growth of RTO-deficient mutants was monitored under the FL
304 20/500 regime for several days. No significant differences were observed in the growth of
305 the mutants, compared to WT cells (Fig. 4A). Previously it has been shown and we have
306 also confirmed that the $\Delta cox/cyd$ double mutant is not viable when subjected to a 12 h
307 dark/12 h high light (150 $\mu\text{mol photons m}^{-2} \text{s}^{-1}$) square-wave cycle regime (Lea-Smith et

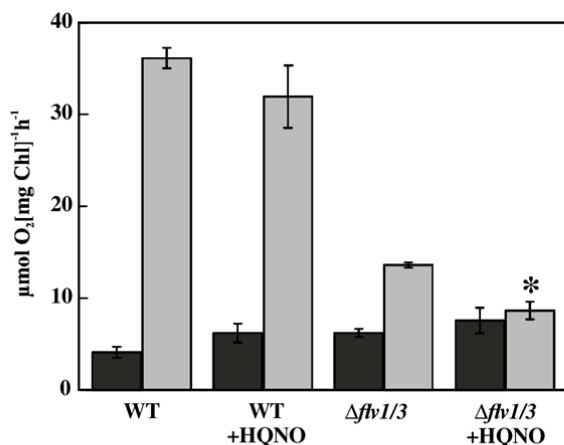


Figure 3. The rates of total O₂ uptake in darkness (black bars) and under the light (grey bars) in the WT and $\Delta fv1/3$ acclimated for 3 days to the fluctuating light FL 20/500 regime (20 $\mu\text{mol photons m}^{-2} \text{s}^{-1}$ background light interrupted by 30-s pulses of 500 $\mu\text{mol photons m}^{-2} \text{s}^{-1}$ light every 5 min). Measurements were performed using MIMS on cells incubated in darkness for 5 min and then illuminated with a strong white light (400 $\mu\text{mol photons m}^{-2} \text{s}^{-1}$) for 5 min either in the absence (control) or in the presence of HQNO. Mean \pm SD, n=3, asterisk indicates statistically significant difference between measurement with HQNO compared to control samples (P<0.05).

308 al., 2013, Fig. S3A). Interestingly, when the duration of alternating dark and high-light
 309 phases was decreased to 5 min (5 min dark/5 min high-light 200 $\mu\text{mol photons m}^{-2} \text{s}^{-1}$) the
 310 $\Delta cox/cyd$ mutant survived (Fig. 4B). However, the growth of this strain and of the Δcox
 311 mutant was slower after 7 days, compared to the WT and Δcyd .

312

313 Gas-exchange analysis of the PS I-less mutant

314 A possible role of RTOs in light-stimulated electron transfer to O₂ in the PS I-less mutant
 315 (Shen et al., 1993), which is lacking functional PS I, was also studied by MIMS gas-
 316 exchange analysis. The ΔPSI cells demonstrated strong light-induced O₂ uptake which was
 317 insensitive to HQNO. However, this could be completely abolished by the addition of
 318 KCN (Fig. 5). These results indicated that in the cells lacking functional PS I, it is not Cyd
 319 but Cox which is shuttling electrons to O₂ during sudden, strong illumination.

320

321 Response of photosynthesis in RTO-deficient mutants to increasing light intensities

322 To characterize the impact of RTOs on photosynthetic electron transfer, “rapid light
 323 curves”, representing the response of photosynthetic parameters to gradually increasing
 324 light intensities, were recorded (Fig. 6). During the experiment the cells were illuminated
 325 with actinic light of different intensities for 60 s and a saturating pulse was applied at the
 326 end of each light period. The effective yield of PS II, Y(II), and the donor side limitation

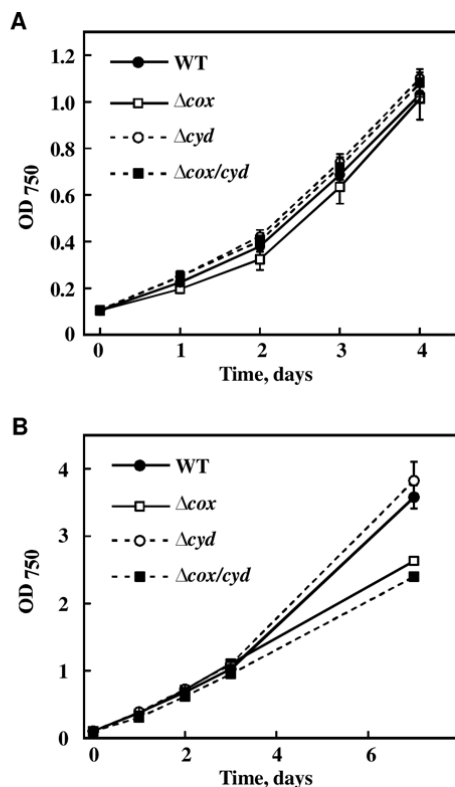


Figure 4. The growth of *Synechocystis* WT and RTO-deficient mutants under: (A) fluctuating light, FL 20/500 (20 $\mu\text{mol photons m}^{-2} \text{s}^{-1}$ background light, interrupted every 5 min with 30 s high light pulses of 500 $\mu\text{mol photons m}^{-2} \text{s}^{-1}$); (B) 5 min dark / 5 min high light (200 $\mu\text{mol photons m}^{-2} \text{s}^{-1}$) square-wave cycles. Mean \pm SD, n=3.

327 of PS I, Y(ND), were specifically addressed to monitor the status of the intersystem
 328 electron transfer chain. The Δcox mutant was similar to the WT in the dynamics of Y(II),
 329 whilst Δcyd and $\Delta\text{cox/cyd}$ demonstrated a decrease of Y(II) under increasing light
 330 intensities (Fig. 6A). In Δcyd cells a decrease in PS II yield was observed under light
 331 intensities ranging from 57 to 220 $\mu\text{mol photons m}^{-2} \text{s}^{-1}$. The $\Delta\text{cox/cyd}$ double mutant
 332 already displayed a decrease in PS II yield at the lower light intensities, starting at 10 μmol
 333 $\text{photons m}^{-2} \text{s}^{-1}$ (Fig. 6A).

334

335 The dynamics of the donor side limitation of PS I, Y(ND), was again similar between WT
 336 and Δcox cells; Y(ND) rose gradually as the light intensity increased (Fig. 6B).
 337 Interestingly, in Δcyd and $\Delta\text{cox/cyd}$ mutant cells, Y(ND) rose faster than in the WT and
 338 significantly exceeded the WT values at 58 $\mu\text{mol photons m}^{-2} \text{s}^{-1}$ (Fig. 6B). However under
 339 higher light intensities, starting from 220 $\mu\text{mol photons m}^{-2} \text{s}^{-1}$, there was a slight but
 340 statistically significant difference ($P < 0.05$) in Y(ND) between Δcyd and $\Delta\text{cox/cyd}$. This
 341 result suggests that under high light the reduced electron flow to P700 in the Δcyd mutant

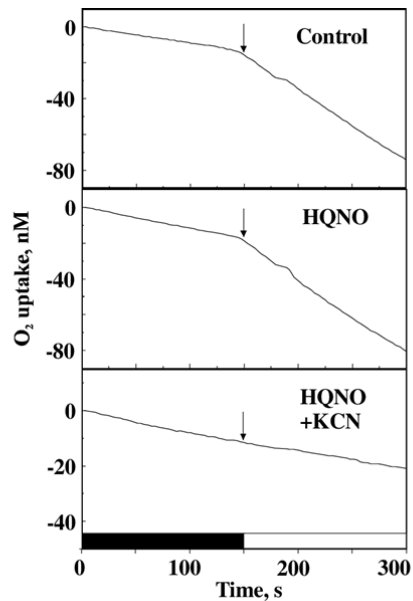


Figure 5. MIMS analysis of O₂ uptake by PS I-less mutant cells in the absence (control) and in the presence of HQNO and HQNO+KCN. O₂ uptake was monitored for 5 min in darkness and 5 min under the light intensity of 150 $\mu\text{mol photons m}^{-2} \text{s}^{-1}$. Arrows indicate the beginning of illumination. The slope of the curves does not provide a precise quantitative measure of the rate of O₂ consumption until it is corrected for the isotopic ratio (¹⁶O/¹⁸O).

342 was presumably due to increased competition for electrons between PS I and Cox. No
 343 significant difference between WT and RTO-mutants was observed in acceptor side
 344 limitation of PS I, Y(NA) (Fig. S4).

345

346 To investigate whether sensitivity of the *Cyd*-deficient mutants to increasing light
 347 intensities would affect the growth of cells under high light, we grew highly diluted
 348 cultures of the WT and RTO-deficient mutants at a continuous light intensity of 500 μmol
 349 $\text{photons m}^{-2} \text{s}^{-1}$ (Fig. S3B). None of the mutants exhibited light-sensitivity under these
 350 conditions and all cultures reached a similar OD₇₅₀ after 2 days of growth.

351

352 **Analysis of the PQ pool redox status in RTO-mutants in darkness**

353 Next we studied the PQ pool redox state in RTO-deficient mutants in darkness and under
 354 far-red (FR) illumination using Chl fluorescence analysis (Fig. 7). The dark-adapted cells
 355 of WT, Δcox and Δcyd demonstrated similar F₀ levels of minimal fluorescence in the dark,
 356 whereas $\Delta\text{cox}/\text{cyd}$ cells had a significantly higher F₀ level (Table S1). Next, a saturating
 357 pulse was applied to the cells to obtain the maximum fluorescence signal in darkness
 358 (F_M^D). All strains demonstrated similar F_M^D values (Table S1). The double mutant retained
 359 a higher level of fluorescence in the dark compared to the WT, whilst the Δcox cells

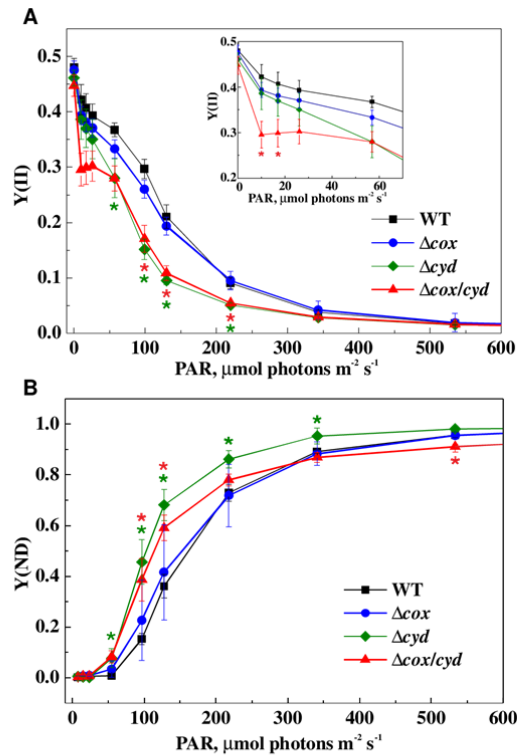


Figure 6. Rapid light curves of the WT and RTO-deficient mutants: (A) PS II yield, Y(II); (B) Donor side limitation of PS I, Y(ND). Mean \pm SD, n=3. Asterisks indicate a statistically significant difference compared to the WT (P<0.05).

360 exhibited a slower relaxation of saturating pulse-induced fluorescence during the
 361 subsequent dark period (Fig. 7).

362

363 Due to the high flow of electrons to the electron transport chain from respiratory
 364 complexes, cyanobacterial cells are usually in State II during dark periods (Mullineaux and
 365 Allen, 1986) and therefore demonstrate low F_M^D values. In order to induce a State II to
 366 State I transition cells were then exposed to FR for 8 s to preferentially excite PS I and
 367 facilitate oxidation of the PQ pool. FR application did not affect the fluorescence level in
 368 the WT and single mutants; however, it resulted in a sudden drop of fluorescence in the
 369 $\Delta\text{cox}/\text{cyd}$ double mutant, to a level just slightly above those of WT and single mutant cells
 370 (Fig. 7). A FR-mediated decrease of fluorescence suggested a highly reduced PQ pool in
 371 $\Delta\text{cox}/\text{cyd}$ cells in darkness, which is in agreement with an earlier study by Howitt *et al*
 372 (2001). When a saturating pulse was applied over a FR background, all strains
 373 demonstrated an increased F_M^{FR} (Fig. 7, Table S1). Afterwards the relaxation of
 374 fluorescence was again recorded in darkness. The fluorescence levels of WT and Δcyd
 375 cells dropped down to a value similar to their initial F_0 levels. The fluorescence signal of

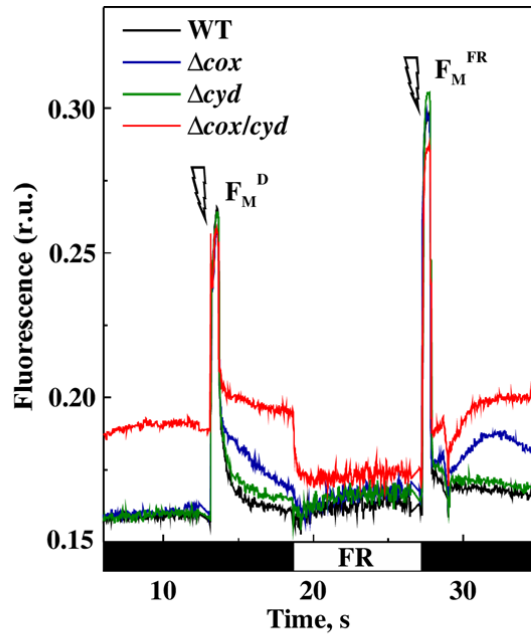


Figure 7. Fluorescence analysis of the WT and RTO-deficient mutant cells. Fluorescence was recorded in darkness (minimal fluorescence, F_0 , black bars on the timescale) and under far-red light (FR). Saturating pulses indicated by flashes were fired to monitor maximum fluorescence level in the dark (F_M^D) and under the FR background (F_M^{FR}). The values are provided in Table S1. Samples were adjusted to a Chl concentration of $15 \mu\text{g mL}^{-1}$ and dark-adapted for 10 min before the measurements. Results of one representative experiment of three independent experiments are shown.

376 the $\Delta\text{cox}/\text{cyd}$ mutant immediately returned to its initial higher level, demonstrating rapid
 377 reduction of the PQ pool in darkness. The Δcox cells demonstrated only a transient
 378 increase and subsequent relaxation of the fluorescence level after the termination of FR
 379 illumination.

380

381 **Characterization of PS II functional status in RTO-mutants**

382 To analyze in detail the functional status of PS II in the RTO mutants, the maximum
 383 quantum yield of PS II (F_V/F_M) was first measured with the Dual-PAM fluorometer in the
 384 presence of DCMU. The values did not differ significantly between the WT and mutants
 385 (Table S1). This is in line with the MIMS data showing nearly similar gross O_2 production
 386 in all studied RTO-deficient mutants compared to the WT (Table 1).

387

388 Next, the status of the PS II acceptor and donor sides in these strains was precisely
 389 addressed by comparing the relaxation kinetics of the flash-induced fluorescence yield.
 390 Following a single-turnover flash, relaxation of the variable fluorescence yield in darkness

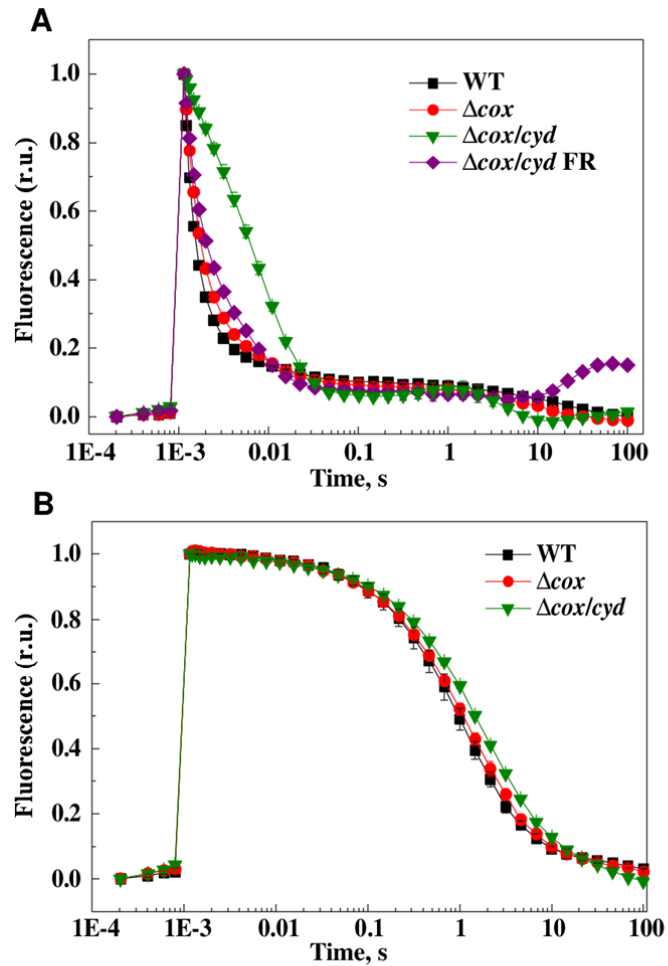


Figure 8. Relaxation of the flash-induced fluorescence yield in darkness. Q_A^- re-oxidation was monitored: (A) from the dark-adapted WT (black squares), Δcox (red circles), $\Delta\text{cox}/\text{cyd}$ (green diamonds) and $\Delta\text{cox}/\text{cyd}$ (purple diamonds) cells pre-illuminated with far-red light for 30 s; (B) in the presence of 20 μM DCMU. Mean \pm SD, $n=3$. The F_0 and F_M values were normalized to 0 and 1, respectively, to facilitate comparison of the kinetics.

391 reflects the Q_A^- re-oxidation via forward Q_A^- -to- Q_B electron transfer and back
 392 recombination with $S_{2/3}$ states of the water-oxidizing complex of PS II. The fluorescence
 393 relaxation kinetics were comparable for WT and Δcyd cells (Fig. S5A), whilst Δcox
 394 showed a slower fluorescence decay and the $\Delta\text{cox}/\text{cyd}$ mutant demonstrated a drastically
 395 slower decay (Fig. 8A). These data indicated modified electron transfer at the PS II
 396 acceptor side in Δcox , which is exacerbated further in the $\Delta\text{cox}/\text{cyd}$ mutant cells.
 397 Interestingly, the fluorescence relaxation curve of $\Delta\text{cox}/\text{cyd}$ displayed a slight “wave
 398 phenomenon”, showing a dip at the time point of approximately 50 ms and a transient rise

399 of fluorescence at about 1 s after the flash. Deák et al. have recently observed similar
400 kinetics of fluorescence relaxation in *Synechocystis* cells when the electron flow to O₂ was
401 inhibited under anoxic conditions (Deák et al., 2014). This was due to transient oxidation
402 of the highly reduced PQ pool by PS I, followed by its re-reduction from cytosolic
403 components via the NDH-1 complex.

404

405 In order to clarify whether the slower relaxation kinetics of the Δcox and $\Delta\text{cox}/\text{cyd}$ mutants
406 were due to a reduced PQ pool, or to structural modifications in the PS II complex, strong
407 FR illumination was applied to cells just before fluorescence measurements. Pre-
408 illumination of the $\Delta\text{cox}/\text{cyd}$ cells with FR, preferentially exciting PS I and thus oxidizing
409 the PQ pool, significantly accelerated the fluorescence decay, bringing the curve closer to
410 that of Δcox cells (Fig. 8A). However, after 10 s of darkness the fluorescence level of the
411 $\Delta\text{cox}/\text{cyd}$ cells again started to increase. These results strongly suggest that a slowdown of
412 the Q_A re-oxidation rate in $\Delta\text{cox}/\text{cyd}$ was predominantly due to a highly reduced PQ pool
413 in darkness. However, FR illumination did not significantly affect the fluorescence
414 relaxation kinetics of the Δcox cells (Fig. S5B).

415

416 In the presence of DCMU, which blocks electron transfer at the Q_B site, Q_A⁻ re-oxidation
417 occurs via charge recombination with the donor side components, mostly the S₂ state of the
418 water oxidizing complex (Vass et al., 1999). Interestingly, in the presence of DCMU,
419 $\Delta\text{cox}/\text{cyd}$ still demonstrated slightly slower fluorescence relaxation, compared to the WT,
420 likely indicating accumulation of PS II centers with a modified donor side in the mutant
421 cells. The Δcox and Δcyd cells showed a similar relaxation kinetics profile to the WT (Fig.
422 8B).

423

424 **The P700 redox state in the RTO-deficient mutants**

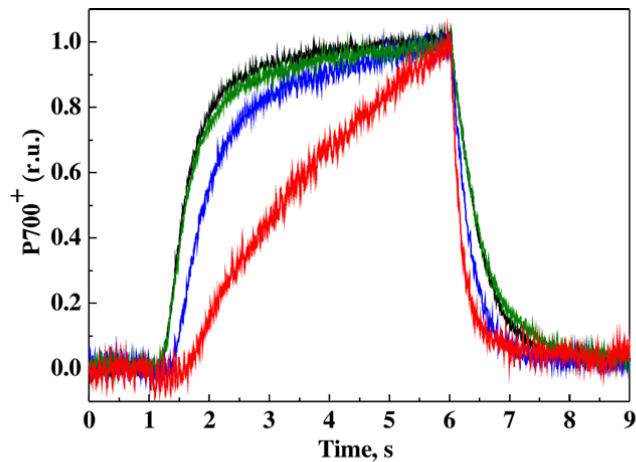


Figure 9. P700 oxido-reduction. P700 oxidation and re-reduction in the WT and mutant cells illuminated with strong far-red light for 5 s. WT (black); Δcox (blue); Δcyd (green); $\Delta\text{cox}/\text{cyd}$ (red). Curves were normalized to the same amplitude to facilitate comparison of the kinetics. Results of one representative experiment of three independent experiments are shown.

425 The redox state of P700 was monitored during dark-light-dark transitions by the
 426 application of strong FR light (Fig. 9). The kinetics of P700 oxidation and re-reduction
 427 were similar between WT and Δcyd cells. The Δcox mutant demonstrated a small lag-
 428 phase during oxidation of P700 and faster re-reduction compared to the WT. Drastically
 429 slower oxidation and faster re-reduction was recorded for the $\Delta\text{cox}/\text{cyd}$ mutant, as
 430 compared to the WT and single mutants (Fig. 9). This is in line with the fluorescence
 431 analysis results, implying a highly reduced PQ pool in $\Delta\text{cox}/\text{cyd}$ cells in darkness.
 432 However, the maximum amount of oxidizable P700 (P_M) did not differ significantly
 433 between the WT and RTO-deficient mutants (Table S1).

434

435 **The PS II/PS I ratio in the RTO-deficient mutants**

436 In order to determine whether the modified redox state of the PQ pool observed in the
 437 double mutant during dark-to-light transitions affected energy transfer between
 438 photosystems, the 77K fluorescence emission spectra of the WT and RTO-deficient
 439 mutants was analyzed. Spectra of mutant cells excited with either 440-nm (Chl excitation)
 440 or 580-nm (phycobilisome excitation) light did not differ from the WT spectra (Fig. S6),
 441 suggesting the absence of significant changes in the PS II/PS I ratio and in energy transfer
 442 from phycobilisomes to the reaction centers of photosystems. In addition, total protein
 443 fractions were isolated from the cells grown under continuous light ($50 \mu\text{mol photons m}^{-2}$
 444 s^{-1}) and probed with a range of antibodies. The amount of PsaB and PsbA (D1), proteins in

445 the reaction centers of PS I and PS II, respectively, were similar between all strains (Fig.
446 S7). Likewise amounts of the ATP synthase β subunit and Flv2, Flv3 and Flv4 were
447 similar between all strains.

448

449

450 **DISCUSSION**

451 The intersystem electron transport chain of photosynthetic organisms plays an important
452 role in regulation of the photosynthetic apparatus. The Cyt *b₆f* complex in higher plants is
453 known to act in photosynthetic control, regulating electron flow to PS I (Nishio and
454 Whitmarsh, 1993; Joliot and Johnson, 2011; Suorsa et al., 2013). In *Synechocystis*, the
455 presence of thylakoid membrane-localized terminal oxidases, Cyd and Cox, strongly
456 suggests that RTOs may regulate the intersystem electron transport, not only under dark
457 conditions, but also during light periods. In *Synechocystis*, the total O₂ uptake in the light
458 could consist of two components: the “respiratory component” and the light-induced
459 component. The “respiratory component” can be detected in darkness but could also
460 contribute to the total O₂ uptake observed under light, whereas the light-induced
461 component can only be monitored upon the application of light and is estimated by
462 subtracting the “respiratory component” from total O₂ uptake under light. Shifting cells
463 from darkness to dim light is known to inhibit O₂ uptake by RTOs (Kok effect), likely
464 because of higher affinity of PS I for electrons from Pc and Cyt *c₆* (Kok, 1949). However,
465 accurately determining the contribution of specific respiratory RTOs to the total O₂ uptake
466 under moderate or high light is a challenge, mainly because it is not known how their
467 relative activity changes under different conditions.

468

469 **Cyd contributes to the redox poise of the PQ pool under light**

470 It was generally accepted that addition of DBMIB should maintain a reduced PQ pool
471 during periods of illumination by blocking electron transport at the site of Cyt *b₆f* (Trebst
472 et al., 1970; Yan et al., 2006). Therefore, in numerous studies, DCMU or DBMIB was
473 added to cyanobacterial cells in order to simulate either an oxidized or reduced redox state
474 of the PQ pool (Hihara et al., 2003; Huang et al., 2003). However, recent data obtained via
475 HPLC demonstrated that in WT *Synechocystis* cells the PQ pool is not as highly reduced
476 during illumination in the presence of DBMIB as previously thought (Schuurmans et al.,
477 2014). Here we demonstrate that, following inhibition of linear electron transport with
478 DBMIB, WT cells of *Synechocystis* are capable of light-induced O₂ uptake, indicating the
479 presence of an alternative electron exit route from the PQ pool to O₂ in the light (Fig. 2).
480 Observed stimulation of O₂ reduction in the light was completely missing after the addition
481 of HQNO to DBMIB treated WT and Δ *cox* cells as well as in the Δ *cyd* and Δ *cox/cyd* cells
482 subjected to DBMIB only (Fig. 2, Table 1). Thus, Cyd contributes to the light-induced O₂
483 uptake observed in the WT when linear electron transport is limited.

484

485 Earlier studies already suggested that Cyd is involved in oxidation of the PQ pool
486 (Schneider et al., 2001; Berry et al., 2002; Schneider et al., 2004). However, those studies
487 were based on an indirect fluorescence method. Through application of the $^{18}\text{O}_2$ isotope
488 and the MIMS technique, we could directly demonstrate the O_2 uptake activity of Cyd
489 (Fig. 2) and also confirmed that Cyd accepts electrons directly from the PQ pool, since the
490 addition of DCBQ eliminated Cyd-mediated light-induced O_2 uptake (Fig. S2A). In the
491 presence of DBMIB, the rates of total O_2 uptake in the light were similar to the rates of
492 gross O_2 production by PS II. Therefore the rate of net photosynthesis was close to zero in
493 the WT and single mutants (Table 1). Importantly, the gross O_2 production rates were
494 about four times higher in the WT and Δcox cells compared to the Δcyd and $\Delta\text{cox}/\text{cyd}$
495 suggesting that the quinol-oxidizing activity of Cyd contributes to alleviation of PS II
496 acceptor side limitation and facilitates gross O_2 production in the presence of DBMIB.
497 This is corroborated by earlier reports which demonstrated an increased level of Cyd
498 associated with impairment of the Cyt *b₆f* complex in the mutants lacking LepB1 and
499 PetC1 (Zhang et al., 2013; Tsunoyama et al., 2009).

500

501 A decrease of the effective PS II yield in the Δcyd and $\Delta\text{cox}/\text{cyd}$ mutant cells upon a
502 sudden increase in light intensity indicates, that in the absence of Cyd, electrons
503 accumulate in the PQ pool and affect the Y(II) levels (Fig. 6A). These data also
504 demonstrate that PQH₂ oxidation by Cyt *b₆f* is the rate-limiting step in the linear electron
505 transport under sub-optimal conditions. Conservation of the PQH₂ oxidizing terminal
506 oxidases, either Cyd, ARTO or PTOX, in all sequenced cyanobacteria which are
507 potentially exposed to high light, further emphasizes the importance of an alternative
508 electron exit pathway to that provided by Cyt *b₆f* (Lea-Smith et al., 2013). An example
509 occurs in the marine cyanobacterium, *Synechococcus* WH8102, which exhibits a
510 significant flow of electrons to O_2 , likely via PTOX, and is caused by the highly reduced
511 state of the PQ pool due to the shortage of Cyt *b₆f* and PS I in an iron-limited environment
512 (Bailey et al., 2008). Moreover, Δcyd develops high PS I donor side limitation more
513 rapidly under elevated light intensities (Fig. 6B), due to up-regulated Cox activity, as is
514 shown by the increased light-induced O_2 uptake rate in this strain (Table 1). Previous
515 studies also suggest that the activity of RTOs in the light might be regulated by the redox

516 state of Pc and Cyt *c* (in the case of Cox) and, plausibly, by the redox state of the PQ pool
517 (in the case of Cyd, PTOX and possibly ARTO) (Ardelean and Peschek, 2011).

518

519 **Interplay between Cyd and flavodiiron proteins**

520 It is clear that both Flv1 and Flv3 are responsible for the light-induced O₂ uptake in
521 *Synechocystis* at least during dark to high light transitions (Fig. S1, Helman et al., 2003;
522 Allahverdiyeva et al., 2011). Helman et al. (2005) estimated that in low CO₂-grown cells
523 of $\Delta flv3$, RTOs redirect 6% of electrons originating from water splitting to O₂ in the light.
524 Thus, upon application of strong light, the mutant retains the “respiratory component” of
525 O₂ uptake driven by RTOs as an alternative sink for light-driven electrons. In agreement
526 with this, under fluctuating light conditions, where electron transfer chain is drastically
527 inhibited in $\Delta flv1/3$ due to damage to PS I (Allahverdiyeva et al., 2013), the $\Delta flv1/3$ mutant
528 showed an HQNO-sensitive light-induced O₂ uptake (Fig. 3). This is yet another
529 demonstration of Cyd-driven light-induced O₂ uptake when cells are grown under sub-
530 optimal conditions, despite the absence of changes in *cyd* transcript level under FL
531 (Mustila et al., 2016).

532

533 It has been previously reported that light-induced O₂ uptake in the $\Delta flv1/3$ cells under FL
534 was functioning at full capacity when cells were exposed to background dim light (20
535 $\mu\text{mol photons m}^{-2} \text{ s}^{-1}$), and that this did not increase further upon the application of high-
536 light pulses. Therefore, Cyd cannot rescue the fatal $\Delta flv1/3$ phenotype (Allahverdiyeva et
537 al., 2013). The unambiguous importance of Flv1 and Flv3 under fluctuating light indicates
538 that they are functioning on a fast time scale downstream of PS I, and have a higher
539 capacity as an electron sink under these conditions, compared to the RTOs. In part this
540 could be due to the soluble nature of Flv1 and Flv3, which would facilitate rapid
541 association with NADPH and allow large amounts of protein to accumulate in the cytosol.
542 In contrast, RTOs are membrane-localized and may be limited in number, due to the
543 highly crowded nature of the thylakoid membrane. Following rapid light changes, a time
544 consuming redistribution of protein complexes occurs within the membrane in order to
545 facilitate efficient electron transfer (Mullineaux, 2014b; Liu et al., 2012).

546

547 **Cox is mostly active in dark respiration, and can be substituted by Cyd under light**
548 **conditions**

549 The contribution of Cyd to dark respiration seems to be minor, since the redox state of the
550 PQ pool in Δcyd cells was not affected in darkness, as confirmed via P700 oxido-reduction
551 (Fig. 9), Q_A^- re-oxidation kinetics (Fig. 8, Fig. S5), and fluorescence analysis (Fig. 7).
552 However, the presence of Cyd was beneficial in Δcox cells under light, since the Q_A^- re-
553 oxidation and the P700 oxido-reduction kinetics differed significantly between Δcox and
554 $\Delta cox/cyd$ cells (Fig. 8, Fig. 9). In contrast to Δcyd , deletion of Cox drastically decreased
555 the rate of dark respiration (Table 1; Howitt and Vermaas, 1998; Pils et al., 1997; Pils and
556 Schmetterer, 2001) and had a prominent effect on the redox state of the PQ pool in
557 darkness (Fig. 7, Fig. 8, Fig. 9), but not under illumination (Fig. 6). Therefore, in
558 *Synechocystis*, Cox can be efficiently substituted by Cyd under illumination. Nevertheless,
559 in the PS I-less mutant of *Synechocystis*, Cox instead of Cyd was the main RTO shuttling
560 electrons to O_2 in the light (Fig. 5). Since Cox is required for chemoheterotrophic growth
561 of *Synechocystis* (Pills et al., 1997) and the PS I-less mutant grows in the presence of
562 glucose under a low light intensity of $5 \mu\text{mol photons m}^{-2} \text{s}^{-1}$, it is highly possible that Cox
563 is the main thylakoid-localized RTO in this mutant. However, since the PS I-less mutant is
564 highly sensitive to light (Shen et al., 1993), the contribution of Cox as an electron shuttle
565 to O_2 is likely to be less efficient compared with PSI activity or this could be a transient
566 phenomenon. It is possible that under specific conditions Cox also produces ROS via a
567 mechanism similar to PTOX in plants (Heyno et al., 2009; Feilke et al. 2014; Yu et al.
568 2014), thereby generating oxidative damage to the cells. On the other hand, rapid light
569 curve analysis demonstrated a slight but significant difference in Y(ND) values between
570 Δcyd and $\Delta cox/cyd$ cells under higher light intensities indicating competition between PS I
571 and Cox for electrons in the Δcyd mutant (Fig 6B). Thus, both Cyd and Cox have a role in
572 regulating the amount of electrons arriving to PS I in the light, although Cox activity only
573 increases only in the absence of Cyd.

574

575 **The role of RTOs in dark/light transitions**

576 Despite strong evidence for thylakoid-based RTOs regulating photosynthetic electron
577 flow, deletion mutants do not demonstrate a strong photoautotrophic growth phenotype
578 under continuous moderate light (Howitt and Vermaas, 1998; Lea-Smith et al., 2013), high
579 light (Fig. S3B, Lea-Smith et al., 2013) and fluctuating light intensity regimes (Fig. 4A).
580 Thus, it is likely that when the Flv1/3 complex is functioning properly under illumination,
581 RTOs are not essential. However, during periods of darkness, only RTOs can oxidize the

582 PQ pool, as demonstrated by the $\Delta\text{cox}/\text{cyd}$ mutant having a drastically slower oxidation
583 and faster re-reduction rate of P700, and slower Q_A^- re-oxidation kinetics in the dark (Fig.
584 7, Fig. 8, Fig. 9). Importantly, the PQ pool in the double mutant could be immediately
585 oxidized by the application of strong FR light (Fig. 7, Fig. 8) but not by the application of
586 low light. The latter result could be concluded from a decreased Y(II) in the light curve
587 analysis at 10-30 $\mu\text{mol photons m}^{-2} \text{ s}^{-1}$ light intensity (Fig. 6A). However, in the same
588 experiment under moderate and high light intensities, $\Delta\text{cox}/\text{cyd}$ behaved similarly to the
589 Δcyd cells.

590

591 Either Cox or Cyd is required for survival of cells under 12 h high light/12 h dark square-
592 wave cycles (Fig. S3A, Lea-Smith et al., 2013) but interestingly not under 12 h high
593 light/12 h dark sinusoidal-wave cycles (Lea-Smith et al., 2013) or 5 min high light/5 min
594 dark square-wave cycles (Fig. 4B). Therefore, the importance of RTOs seems to depend on
595 both the length of the dark and light periods and the amount of photodamage occurring
596 during the light period. Indeed, significant ROS production and inactivation of the PS II
597 complex was observed in the double mutant subjected to 12 h high light/12 h dark square-
598 wave cycles only at the end of a long dark period, possibly due to an insufficient amount
599 of ATP for PS II repair and an over-reduced PQ pool (Lea-Smith et al., 2013). Under 12 h
600 high light/12 h dark sinusoidal-wave cycles, (i) cells are not subjected to rapid high light
601 exposure, reducing damage to PS II, moreover (ii) damaged PS II centers have a
602 possibility for efficient repair during a low light phase before a dark period, therefore the
603 cells have a reduced energy requirements for repair, which can be substituted by
604 alternatives to dark respiration, most likely fermentation.

605

606 Under short dark/light periods (Fig. 4B) the cells may be able to oxidize the PQ pool
607 regularly, thus generating ATP and reducing power which can be used in darkness,
608 although not as efficiently as the WT, since growth of the Δcox and $\Delta\text{cox}/\text{cyd}$ mutants was
609 reduced after 7 days.

610

611 **CONCLUSION**

612 Through the use of well-defined mutants and inhibitors combined with MIMS gas-
613 exchange analysis, we show the subtle effects of loss of RTO complexes on each part of
614 the photosynthetic electron transfer chain. Importantly, RTO-mediated respiratory O_2

615 uptake can continue at a similar rate upon high light illumination, thus contributing to
616 oxidation of the PQ pool. Cox is the most important RTO in dark respiration, but also
617 competes with PS I for electrons, functioning as a regulator of the electron flow to this
618 photosystem under high light. Under illumination, Cyd is the major RTO oxidizing PQH₂.
619 However, Cyd only up-regulates O₂ photoreduction under certain conditions, specifically
620 when Flv1 and Flv3 protein activity is insufficient to prevent linear electron transport
621 blockage at the level of Cyt *b₆f* or PS I. Flv1 and Flv3 proteins are not involved in dark
622 respiration but are responsible for the majority of the light-induced O₂ uptake component.
623 Thus both RTOs and Flv1/3 pathways play an important role in alleviation of excess
624 electrons using O₂ as a terminal acceptor under illumination: RTOs continue to function in
625 the light, although operating on slower time ranges and on limited scale, whereas Flv1/3
626 responds rapidly as a light-induced component and with greater capacity.

627

628

629 **MATERIALS AND METHODS**

630

631 **Strains and Culture Conditions**

632 The strains used in this study included *Synechocystis* sp. PCC 6803 (WT), mutants lacking
633 respiratory terminal oxidases: Δcyd , Δcox , $\Delta cox/cyd$ (all described previously in Lea-Smith
634 et al., 2013); mutant deficient in flavodiiron proteins: $\Delta flv1/flv3$ (Allahverdiyeva et al.,
635 2011) and the PS I-less mutant (Shen et al., 1993). Cells were maintained in BG11
636 medium buffered with 10mM N-[Tris(hydroxymethyl)methyl]-2-aminoethanesulfonic acid
637 (TES-KOH, pH 8.2) under continuous illumination of 50 $\mu\text{mol photons m}^{-2} \text{s}^{-1}$ (PAR), 3%
638 CO₂, 30 °C with gentle agitation (120 rpm). For all physiological experiments cells were
639 inoculated to OD_{750nm}=0.5-0.6 and shifted to ambient CO₂ conditions for 3 days before
640 measurements. Experimental cultures were cultivated in AlgaeTron AG130 growth
641 chambers (PSI Instruments, Czech) under continuous illumination of 50 $\mu\text{mol photons m}^{-2}$
642 s^{-1} (provided by cool-white LED), unless mentioned otherwise. For the high light growth
643 experiments, a dilution series of cells starting from OD₇₅₀=0.1 were subjected to a light
644 intensity of 500 $\mu\text{mol photons m}^{-2} \text{s}^{-1}$. For the MIMS measurements of fluctuating light-
645 treated cells, cultures at an OD₇₅₀=0.5-0.6 were shifted to a light regime with a background
646 light of 20 $\mu\text{mol photons m}^{-2} \text{s}^{-1}$ interrupted by 30 s pulses of 500 $\mu\text{mol photons m}^{-2} \text{s}^{-1}$
647 light every 5 min (FL 20/500). For the growth experiments under fluctuating light

648 conditions, cells were subjected to FL 20/500 or a 5 min dark/5 min 200 $\mu\text{mol photons m}^{-2}$
649 s^{-1} light regime starting from an $\text{OD}_{750}=0.1$. For all activity measurements, cells were
650 harvested and resuspended in fresh BG11 medium at the desired Chl concentration and
651 acclimated for 1 h under respective growth conditions before the measurements. The PS I-
652 less mutant was grown in the presence of 5 mM glucose at a light intensity of 5 μmol
653 $\text{photons m}^{-2} \text{s}^{-1}$.

654

655 **Membrane Inlet Mass Spectrometry (MIMS)**

656 Online measurements of $^{16}\text{O}_2$ (mass 32) production and $^{18}\text{O}_2$ (mass 36) consumption were
657 monitored using mass spectrometry (model Prima PRO, Thermo Scientific). The
658 membrane inlet system consists of a thermo-regulated DW1 oxygen electrode chamber,
659 which is connected to the vacuum line of the mass spectrometer via a gas-permeable thin
660 Teflon membrane (1 mil stretch membrane, YSI Inc, Ohio, USA), which seals the bottom
661 of the chamber. For analyses, 1.5 ml of cell suspension at a Chl concentration of 15 μg
662 mL^{-1} was placed into the measuring chamber and stirred continuously. Gases dissolved in
663 the medium diffuse through the Teflon membrane to the ion source of the mass
664 spectrometer. Prior to the measurement, $^{18}\text{O}_2$ (isotope purity > 98%; CK Gas Products Ltd)
665 was injected by bubbling at the top of the suspension until the concentrations of $^{16}\text{O}_2$ and
666 $^{18}\text{O}_2$ were equal. Then samples were measured for 5 min in darkness to record O_2
667 consumption caused by respiration. Following this period, actinic light (400 $\mu\text{mol photons}$
668 $\text{m}^{-2} \text{s}^{-1}$; 150 $\mu\text{mol photons m}^{-2} \text{s}^{-1}$ in the case of the PS I-less mutant) was applied via a
669 150 Watt, 21 V, EKE quartz halogen-powered fiber optic illuminator (Fiber-Lite DC-950,
670 Dolan-Jenner, MA, USA). Gas-exchange kinetics and rates were determined according to
671 Beckmann et al. (2009). The final concentration of inhibitors and electron acceptors used
672 in MIMS experiments was 25 μM DBMIB, 50 μM HQNO, 0.5 mM DCBQ and 1 mM
673 KCN. All the measurements were performed in the presence of 1 mM NaHCO_3 .

674

675 **Protein Isolation, Electrophoresis, and Immunodetection**

676 Total protein extracts of *Synechocystis* cells were isolated as described in Zhang et al.
677 (2009). Proteins were separated by 12% (w/v) SDS-PAGE containing 6 M urea,
678 transferred to a PVDF membrane (Immobilon-P, Millipore) and analyzed with the protein-
679 specific antibodies.

680

681 **Fluorescence measurements**

682 The Chl fluorescence from intact cells was recorded with a pulse amplitude modulated
683 fluorometer Dual-PAM-100 (Walz, Germany). Prior to measurements, cell suspensions at
684 a Chl concentration of $15 \mu\text{g mL}^{-1}$ were dark-adapted for 10 min. Saturating pulses of
685 $5,000 \mu\text{mol photons m}^{-2} \text{ s}^{-1}$ (300 ms) and strong far-red light (720 nm , 75 W m^{-2}) were
686 applied to samples when required. The maximum quantum yield of PS II was calculated as
687 $(F_M - F_0)/F_M = F_V/F_M$, and measured in the presence of $20 \mu\text{M}$ DCMU from dark-adapted
688 cells upon the application of red actinic light of $200 \mu\text{mol photons m}^{-2} \text{ s}^{-1}$ for 1 min.

689

690 The kinetics of the Chl fluorescence decay after a single-turnover saturating flash were
691 monitored using a fluorometer FL 3500 (PSI Instruments) according to Vass et al. (1999).
692 Cells were adjusted to a Chl concentration of $7.5 \mu\text{g mL}^{-1}$ and dark-adapted for 5 min
693 before measurements. When indicated, measurements were performed in the presence of
694 $20 \mu\text{M}$ DCMU. In some experiments cells were illuminated for 30 s with a strong far-red
695 light before application of the flash.

696

697 The fluorescence emission spectra at 77K were measured from intact cells using a
698 USB4000-FL-450 (Ocean Optics) spectrofluorometer. Samples were removed from
699 cultures, adjusted to a Chl concentration of $7.5 \mu\text{g mL}^{-1}$, rapidly frozen in liquid nitrogen
700 and excited with 580 nm or 440 nm light generated with interference filters 10 nm in
701 width.

702

703 **P700 Oxidation and Re-reduction**

704 Oxidation and re-reduction of P700 was monitored using a Dual-PAM-100 (Walz). Cell
705 suspensions at a Chl concentration of $20 \mu\text{g mL}^{-1}$ were dark-adapted for 2 min before
706 measurements. For P700 oxidation, cells were illuminated with strong far-red light (720
707 nm , 75 W m^{-2}) for 5 s and the subsequent re-reduction was recorded in darkness.

708

709 **Light Curves**

710 Rapid light curves were measured without dark adaptation of the cells using standard
711 protocols programmed into a Dual-PAM-100 (Walz) with the 60 s illumination periods
712 gradually increasing in light intensity. At the end of each light period a saturating pulse
713 was applied to monitor the photosynthetic parameters. The effective yield of PS II, $Y(\text{II})$,

714 was calculated as $(F_M' - F_S)/F_M'$. The Y(ND), non-photochemical quantum yield of PS I
 715 caused by the donor side limitation, was calculated as (P/P_M) . The Y(NA), acceptor side
 716 limitation of PS I, was calculated as $[(P_M - P_M') / P_M]$.

717

718 **Acknowledgments:** We are grateful to Dr. W. Vermaas for sharing the PS I-less mutant.

719

720

721 **Table 1.** O₂ exchange rates of the WT and mutant cells. Rates are in $\mu\text{mol O}_2 [\text{mg Chl}]^{-1} \text{h}^{-1}$
 722 ¹. Mean \pm SD, n=3-5. Asterisks indicate a statistically significant difference compared to
 723 the WT (P<0.05).

| Gas-exchange conditions | | | WT | Δcyd | Δcox | $\Delta\text{cox}/\text{cyd}$ |
|-------------------------|---------------------------|---------------|------------------|--------------------|--------------------|-------------------------------|
| Control | O ₂ uptake | Dark | 8.3 \pm 1.2 | 5.1 \pm 0.8* | 3.5 \pm 0.5* | 0.3 \pm 0.2* |
| | | Light-induced | 26.3 \pm 6.9 | 35.3 \pm 8.3* | 38.4 \pm 5.5* | 24.7 \pm 3.0 |
| | | Total Light | 34.6 \pm 6.7 | 40.5 \pm 7.5 | 41.5 \pm 5.1* | 24.9 \pm 3.0 |
| | O ₂ production | Gross | 193.3 \pm 20.1 | 190.7 \pm 26.4 | 190.25 \pm 18.1 | 184.9 \pm 21.5 |
| | | Net | 158.6 \pm 19.3 | 150.3 \pm 19.2 | 148.7 \pm 15.1 | 159.6 \pm 22.5 |
| DBMIB | O ₂ uptake | Dark | 10.1 \pm 1.5 | 13.1 \pm 1.3 | 12.8 \pm 3.1 | 9.3 \pm 1.3 |
| | | Light-induced | 11.6 \pm 2.3 | N/A | 7.9 \pm 0.6 * | N/A |
| | | Total Light | 21.5 \pm 2.8 | 7.0 \pm 0.8* | 20.7 \pm 2.5 | 7.7 \pm 1.9* |
| | O ₂ production | Gross | 24.2 \pm 3.1 | 5.5 \pm 1.3* | 19.8 \pm 3.8* | 2.75 \pm 0.4* |
| | | Net | 2.9 \pm 0.2 | N/A | N/A | N/A |
| DBMIB+ HQNO | O ₂ uptake | Dark | 12.9 \pm 0.3 | 11.3 \pm 3.5 | 10.9 \pm 3.9 | 10.2 \pm 0.2* |
| | | Light-induced | N/A | N/A | N/A | N/A |
| | | Total Light | 12.3 \pm 0.6 | 7.0 \pm 1.1 | 10.8 \pm 3.4 | 9.8 \pm 0.5 |

724

725 **Figure Legends**

726 **Figure 1.** Schematic diagram of the thylakoid membrane-localized photosynthetic and
 727 respiratory electron transfer chains. Lines indicate electron transport; dotted lines indicate
 728 possible but poorly characterized electron transfer and proton pathways. PS II,
 729 Photosystem II; Flv2/4, Flavodiiron proteins 2/4; Flv1/3, Flavodiiron proteins 1/3; PQ,
 730 plastoquinone; PQH₂, plastoquinol; Cyt *b*₆f, cytochrome *b*₆f complex; Pc, plastocyanin;
 731 Cyt *c*₆, cytochrome *c*₆; PS I, Photosystem I; Fd, ferredoxin; FNR, ferredoxin-NADP⁺
 732 oxidoreductase; NDH-1, NAD(P)H dehydrogenase-like complex type 1; SDH, succinate

733 dehydrogenase; NDH-2, NAD(P)H dehydrogenase type 2; Cyd, cytochrome *bd* quinol
734 oxidase; Cox, cytochrome *c* oxidase.

735

736 **Figure 2.** The rates of O₂ exchange in the WT and Δ *cyd* mutant cells incubated in darkness
737 for 5 min and then illuminated with a strong white light (400 μ mol photons m⁻² s⁻¹) for the
738 next 5 min. Black bars and grey bars indicate the rates of total O₂ uptake by cells in
739 darkness and in the light, respectively; white bars indicate the gross O₂ production rate.
740 Measurements were performed either in the absence of inhibitors (control) or in the
741 presence of DBMIB or DBMIB + HQNO. Mean \pm SD, n=3-5.

742

743 **Figure 3.** The rates of total O₂ uptake in darkness (black bars) and in the light (grey bars)
744 in the WT and Δ *flv1/3* acclimated for 3 days to a fluctuating light FL 20/500 regime
745 (20 μ mol photons m⁻² s⁻¹ background light interrupted by 30 s pulses of 500 μ mol photons
746 m⁻² s⁻¹ light every 5 min). Measurements were performed using MIMS on cells incubated
747 in darkness for 5 min and then illuminated with a strong white light (400 μ mol photons m⁻²
748 s⁻¹) for 5 min either in the absence (control) or in the presence of HQNO. Mean \pm SD, n=3,
749 asterisks indicates statistically significant difference between measurement with HQNO
750 compared to control samples (P<0.05).

751

752 **Figure 4.** The growth of *Synechocystis* WT and RTO-deficient mutants under: (A)
753 fluctuating light, FL 20/500 (20 μ mol photons m⁻² s⁻¹ background light, interrupted every
754 5 min with 30 s high light pulses of 500 μ mol photons m⁻² s⁻¹); (B) 5 min dark / 5 min
755 high light (200 μ mol photons m⁻² s⁻¹) square-wave cycles. Mean \pm SD, n=3.

756

757 **Figure 5.** MIMS analysis of O₂ uptake by PS I-less mutant cells in the absence (control)
758 and in the presence of HQNO and HQNO+KCN. O₂ uptake was monitored for 5 min in
759 darkness and 5 min under a light intensity of 150 μ mol photons m⁻² s⁻¹. Arrows indicate the
760 beginning of illumination. The slope of the curves does not provide a precise quantitative
761 measure of the rate of O₂ consumption until it is corrected for the isotopic ratio (¹⁶O/¹⁸O).

762

763 **Figure 6.** Rapid light curves of the WT and RTO-deficient mutants: (A) PS II yield, Y(II);
764 (B) Donor side limitation of PS I, Y(ND). Mean \pm SD, n=3. Asterisks indicate a
765 statistically significant difference compared to WT (P<0.05).

766 **Figure 7.** Fluorescence analysis of the WT and RTO-deficient mutant cells. Fluorescence
767 was recorded in darkness (minimal fluorescence, F_0 , black bars on the timescale) and
768 under far-red light (FR). Saturating pulses indicated by flashes were fired to monitor
769 maximum fluorescence level in the dark (F_M^D) and under the FR background (F_M^{FR}). The
770 values are provided in Table S1. Samples were adjusted to a Chl concentration of 15 μg
771 mL^{-1} and dark-adapted for 10 min before the measurements. A representative curve of
772 three independent experiments is shown.

773

774 **Figure 8.** Relaxation of the flash-induced fluorescence yield in darkness. Q_A^- re-oxidation
775 was monitored: (A) from the dark-adapted WT (black squares), Δcox (red circles),
776 $\Delta\text{cox}/\text{cyd}$ (green diamonds) and $\Delta\text{cox}/\text{cyd}$ (purple diamonds) cells pre-illuminated with far-
777 red light for 30 s; (B) in the presence of 20 μM DCMU. Mean \pm SD, $n=3$. The F_0 and F_M
778 values were normalized to 0 and 1, respectively, to facilitate comparison of the kinetics.

779

780 **Figure 9.** P700 oxido-reduction. P700 oxidation and re-reduction in the WT and mutant
781 cells illuminated with strong far-red light for 5 s. WT (black); Δcox (blue); Δcyd (green);
782 $\Delta\text{cox}/\text{cyd}$ (red). Curves were normalized to the same amplitude to facilitate comparison of
783 the kinetics. A representative curve of three independent experiments is shown.

784

785

786

Parsed Citations

Abramson J, Riistama S, Larsson G, Jasaitis A, Svensson-Ek M, Laakkonen L, Puustinen A, Iwata S, Wikström M (2000) The structure of the ubiquinol oxidase from Escherichia coli and its ubiquinone binding site. Nat Struct Biol 7: 910-917

Pubmed: [Author and Title](#)

CrossRef: [Author and Title](#)

Google Scholar: [Author Only](#) [Title Only](#) [Author and Title](#)

Allahverdiyeva Y, Ermakova M, Eisenhut M, Zhang P, Richaud P, Hagemann M, Cournac L, Aro EM (2011) Interplay between flavodiiron proteins and photorespiration in Synechocystis sp. PCC 6803. J Biol Chem 286: 24007-24014

Pubmed: [Author and Title](#)

CrossRef: [Author and Title](#)

Google Scholar: [Author Only](#) [Title Only](#) [Author and Title](#)

Allahverdiyeva Y, Mustila H, Ermakova M, Bersanini L, Richaud P, Ajani G, Battchikova N, Cournac L, Aro EM (2013) Flavodiiron proteins Flv1 and Flv3 enable cyanobacterial growth and photosynthesis under fluctuating light in aquatic environments. Proc Natl Acad Sci USA 110: 4111-4116

Pubmed: [Author and Title](#)

CrossRef: [Author and Title](#)

Google Scholar: [Author Only](#) [Title Only](#) [Author and Title](#)

Ardelean II, Peschek GA (2011) The Site of Respiratory Electron Transport in Cyanobacteria and Its Implication for the Photo-Inhibition of Respiration In Peschek GA, Obinger C, Renger G, eds, Bioenergetic processes of cyanobacteria - from evolutionary singularity to ecological diversity, Springer, New York, pp 131-136

Bailey S, Melis A, Mackey KR, Cardol P, Finazzi G, van Dijken G, Berg GM, Arrigo K, Shrager J, Grossman A (2008) Alternative photosynthetic electron flow to oxygen in marine Synechococcus. Biochim Biophys Acta 1777: 269-276

Pubmed: [Author and Title](#)

CrossRef: [Author and Title](#)

Google Scholar: [Author Only](#) [Title Only](#) [Author and Title](#)

Beckmann K, Messinger J, Badger M, Wyrzynski T, Hillier W (2009) On-line mass spectrometry: membrane inlet sampling. Photosynth Res 102: 511-522

Pubmed: [Author and Title](#)

CrossRef: [Author and Title](#)

Google Scholar: [Author Only](#) [Title Only](#) [Author and Title](#)

Belatik A, Joly D, Hotchandani S, Carpentier R (2013) Re-evaluation of the side effects of cytochrome b6f inhibitor dibromothymoquinone on photosystem II excitation and electron

transfer. Photosynth Res 117: 489-496

Berry S, Schneider D, Vermaas W, Rogner M (2002) Electron transport routes in whole cells of Synechocystis sp. strain PCC 6803: the role of the cytochrome bd-type oxidase. Biochemistry 41: 3422-3429

Pubmed: [Author and Title](#)

CrossRef: [Author and Title](#)

Google Scholar: [Author Only](#) [Title Only](#) [Author and Title](#)

Bukhov N, Sridharan G, Egorova E, Carpentier R (2003) Interaction of exogenous quinones with membranes of higher plant chloroplasts: modulation of quinone capacities as photochemical and non-photochemical quenchers of energy in Photosystem II during light-dark transitions. Biochim Biophys Acta 1604: 115-123

Pubmed: [Author and Title](#)

CrossRef: [Author and Title](#)

Google Scholar: [Author Only](#) [Title Only](#) [Author and Title](#)

Brändén G, Genniss RB, Brzezinska P (2006) Transmembrane proton translocation by cytochrome c oxidase. Biochim Biophys Acta 1757: 1052-1063

Pubmed: [Author and Title](#)

CrossRef: [Author and Title](#)

Google Scholar: [Author Only](#) [Title Only](#) [Author and Title](#)

Cooley JW, Howitt CA, Vermaas W (2000) Succinate:Quinol oxidoreductases in the cyanobacterium Synechocystis sp. strain PCC 6803: presence and function in metabolism and electron transport. J Bacteriol 182: 714-722

Pubmed: [Author and Title](#)

CrossRef: [Author and Title](#)

Google Scholar: [Author Only](#) [Title Only](#) [Author and Title](#)

Deák Z, Sass L, Kiss E, Vass I (2014) Characterization of wave phenomena in the relaxation of flash-induced chlorophyll fluorescence yield in cyanobacteria. Biochim Biophys Acta 1837: 1522-32

Pubmed: [Author and Title](#)

CrossRef: [Author and Title](#)

Google Scholar: [Author Only](#) [Title Only](#) [Author and Title](#)

Eisenhut M, Kahlon S, Hasse D, Ewald R, Lieman-Hurwitz J, Ogawa T, Ruth W, Bauwe H, Kaplan A, Hagemann M (2006) The plantlike C2 glycolate cycle and the bacterial-like glycerate pathway cooperate in phosphoglycolate metabolism in cyanobacteria. Plant Physiol 142: 333-342

Pubmed: [Author and Title](#)

CrossRef: [Author and Title](#)

Google Scholar: [Author Only](#) [Title Only](#) [Author and Title](#)

Eisenhut M, Ruth W, Haimovich M, Bauwe H, Kaplan A, Hagemann M (2008) The photorespiratory glycolate metabolism is essential for cyanobacteria and might have been conveyed endosymbiontically to plants. *Proc Natl Acad Sci USA* 105: 17199-17204

Pubmed: [Author and Title](#)

CrossRef: [Author and Title](#)

Google Scholar: [Author Only](#) [Title Only](#) [Author and Title](#)

Ermakova M, Battchikova N, Richaud P, Leino H, Kosourov S, Isojärvi J, Peltier G, Flores E, Cournac L, Allahverdiyeva Y, Aro EM (2014) Heterocyst-specific flavodiiron protein Flv3B enables oxic diazotrophic growth of the filamentous cyanobacterium *Anabaena* sp. PCC 7120. *Proc Natl Acad Sci USA* 111: 11205-11210

Pubmed: [Author and Title](#)

CrossRef: [Author and Title](#)

Google Scholar: [Author Only](#) [Title Only](#) [Author and Title](#)

Feilke K, Yu Q, Beyer P, Sétif P, Krieger-Liszskay A (2014) In vitro analysis of the plastid terminal oxidase in photosynthetic electron transport. *Biochim Biophys Acta* 1837: 1684-1690.

Pubmed: [Author and Title](#)

CrossRef: [Author and Title](#)

Google Scholar: [Author Only](#) [Title Only](#) [Author and Title](#)

Graan T, Ort DJ (1986) Detection of oxygen-evolving photosystem II centers inactive in plastoquinone reduction. *Biochim Biophys Acta* 852: 320-330

Pubmed: [Author and Title](#)

CrossRef: [Author and Title](#)

Google Scholar: [Author Only](#) [Title Only](#) [Author and Title](#)

Hart SE, Schlarb-Ridley BG, Bendall DS, Howe CJ (2005) Terminal oxidases of cyanobacteria. *Biochem Soc Trans* 33: 832-835

Pubmed: [Author and Title](#)

CrossRef: [Author and Title](#)

Google Scholar: [Author Only](#) [Title Only](#) [Author and Title](#)

Helman Y, Barkan E, Eisenstadt D, Luz B, Kaplan A (2005) Fractionation of the three stable oxygen isotopes by oxygen-producing and oxygen consuming reactions in photosynthetic organisms. *Plant Physiol* 138: 2292-2298

Pubmed: [Author and Title](#)

CrossRef: [Author and Title](#)

Google Scholar: [Author Only](#) [Title Only](#) [Author and Title](#)

Helman Y, Tchernov D, Reinhold L, Shibata M, Ogawa T, Schwarz R, Ohad I, Kaplan A (2003) Genes encoding A-type flavoproteins are essential for photoreduction of O₂ in cyanobacteria. *Curr Biol* 13: 230-235

Pubmed: [Author and Title](#)

CrossRef: [Author and Title](#)

Google Scholar: [Author Only](#) [Title Only](#) [Author and Title](#)

Heyno E, Gross C, Laureau C, Culcasi M, Pietri S, Krieger-Liszskay A (2009) Plastid Alternative Oxidase (PTOX) Promotes Oxidative Stress When Overexpressed in Tobacco. *J. Biol. Chem.* 284: 31174-31180.

Pubmed: [Author and Title](#)

CrossRef: [Author and Title](#)

Google Scholar: [Author Only](#) [Title Only](#) [Author and Title](#)

Hihara Y, Sonoike K, Kanehisa M, Ikeuchi M (2003) DNA microarray analysis of redox-responsive genes in the genome of the cyanobacterium *Synechocystis* sp. strain PCC 6803. *J Bacteriol* 185: 1719-1725.

Pubmed: [Author and Title](#)

CrossRef: [Author and Title](#)

Google Scholar: [Author Only](#) [Title Only](#) [Author and Title](#)

Howitt C, Cooley J, Wiskich J, Vermaas W (2001) A strain of *Synechocystis* sp. PCC 6803 without photosynthetic oxygen evolution and respiratory oxygen consumption: implications for the study of cyclic photosynthetic electron transport. *Planta* 214: 46-56.

Pubmed: [Author and Title](#)

CrossRef: [Author and Title](#)

Google Scholar: [Author Only](#) [Title Only](#) [Author and Title](#)

Howitt C, Udall P, Vermaas W (1999) Type 2 NADH dehydrogenases in the cyanobacterium *Synechocystis* sp. strain PCC 6803 are involved in regulation rather than respiration. *J Bacteriol* 181: 3994-4003

Pubmed: [Author and Title](#)

CrossRef: [Author and Title](#)

Google Scholar: [Author Only](#) [Title Only](#) [Author and Title](#)

Howitt C, Vermaas WF (1998) Quinol and cytochrome oxidases in the cyanobacterium *Synechocystis* sp. PCC 6803. *Biochemistry* 37: 17944-17951

Pubmed: [Author and Title](#)

CrossRef: [Author and Title](#)

Google Scholar: [Author Only](#) [Title Only](#) [Author and Title](#)

Huang C, Yuan X, Zhao J, Bryant DA (2003) Kinetic analyses of state transitions of the cyanobacterium *Synechococcus* sp. PCC 7002 and its mutant strains impaired in electron transport. *Biochim Biophys Acta* 1607: 121-130

Pubmed: [Author and Title](#)

CrossRef: [Author and Title](#)

Google Scholar: [Author Only](#) [Title Only](#) [Author and Title](#)

Huang F, Parmryd I, Nilsson F, Persson AL, Pakrasi HB, Andersson B, Norling B (2002) Proteomics of *Synechocystis* sp. strain PCC 6803: identification of plasma membrane proteins. *Mol Cell Proteomics* 1: 956-966.

Pubmed: [Author and Title](#)
CrossRef: [Author and Title](#)
Google Scholar: [Author Only](#) [Title Only](#) [Author and Title](#)

Iwata S, Ostermeier C, Ludwig B, Michel H (1995) Structure at 2.8-Angstrom Resolution of Cytochrome-C-Oxidase from Paracoccus-Denitrificans. Nature 376: 660-669

Pubmed: [Author and Title](#)
CrossRef: [Author and Title](#)
Google Scholar: [Author Only](#) [Title Only](#) [Author and Title](#)

Joliot P, Johnson GN (2011) Regulation of cyclic and linear electron flow in higher plants. Proc Natl Acad Sci 108: 13317-13322

Pubmed: [Author and Title](#)
CrossRef: [Author and Title](#)
Google Scholar: [Author Only](#) [Title Only](#) [Author and Title](#)

Kok B (1949) On the interrelation of respiration and photosynthesis in green plants. Biochim Biophys Acta 3: 625-631

Pubmed: [Author and Title](#)
CrossRef: [Author and Title](#)
Google Scholar: [Author Only](#) [Title Only](#) [Author and Title](#)

Kranzler C, Lis H, Finkel OM, Schmetterer G, Shaked Y, Keren N (2014) Coordinated transporter activity shapes high-affinity iron acquisition in cyanobacteria. ISME J 8: 409-417

Pubmed: [Author and Title](#)
CrossRef: [Author and Title](#)
Google Scholar: [Author Only](#) [Title Only](#) [Author and Title](#)

Kufryk G, Vermaas W (2006) Sll1717 in Synechocystis sp. PCC 6803 affects the redox state of the plastoquinone pool by modulating quinol oxidase activity in thylakoids. J. Bacteriol 188: 1286-1294

Pubmed: [Author and Title](#)
CrossRef: [Author and Title](#)
Google Scholar: [Author Only](#) [Title Only](#) [Author and Title](#)

Lea-Smith DJ, Bombelli P, Vasudevan R, Howe C (2016) Photosynthetic, respiratory and extracellular electron transport pathways in cyanobacteria. Biochim Biophys Acta 1857: 247-255

Pubmed: [Author and Title](#)
CrossRef: [Author and Title](#)
Google Scholar: [Author Only](#) [Title Only](#) [Author and Title](#)

Lea-Smith DJ, Ross N, Zori M, Bendall DS, Dennis JS, Scott SA, Smith AG, Howe CJ (2013) Thylakoid terminal oxidases are essential for the cyanobacterium Synechocystis sp. PCC 6803 to survive rapidly changing light intensities. Plant Physiol 162: 484-495

Pubmed: [Author and Title](#)
CrossRef: [Author and Title](#)
Google Scholar: [Author Only](#) [Title Only](#) [Author and Title](#)

Liu LN, Bryan SJ, Huang F, Yu J, Nixon PJ, Rich PR, Mullineaux CW (2012) Control of electron transport routes through redox-regulated redistribution of respiratory complexes. Proc Natl Acad Sci USA 109: 11431-11436

Pubmed: [Author and Title](#)
CrossRef: [Author and Title](#)
Google Scholar: [Author Only](#) [Title Only](#) [Author and Title](#)

Matthijs HC, Lubberding HJ (1988) Dark respiration in cyanobacteria. In LJ Rogers, JR Gallon, eds, Biochemistry of the Algae and Cyanobacteria. Clarendon Press, Oxford, pp 131-145

Pubmed: [Author and Title](#)
CrossRef: [Author and Title](#)
Google Scholar: [Author Only](#) [Title Only](#) [Author and Title](#)

McDonald AE, Ivanov AG, Bode R, Maxwell DP, Rodermeil SR, Huner NP (2011) Flexibility in photosynthetic electron transport: the physiological role of plastoquinol terminal oxidase (PTOX). Biochim Biophys Acta 1807: 954-967

Pubmed: [Author and Title](#)
CrossRef: [Author and Title](#)
Google Scholar: [Author Only](#) [Title Only](#) [Author and Title](#)

Mi H, Endo T, Schreiber U, Ogawa T, Asada K (1992) Electron donation from cyclic and respiratory flows to the photosynthetic intersystem chain is mediated by pyridine nucleotide dehydrogenase in the cyanobacterium Synechocystis PCC 6803. Plant Cell Physiol 33: 1233-1237

Pubmed: [Author and Title](#)
CrossRef: [Author and Title](#)
Google Scholar: [Author Only](#) [Title Only](#) [Author and Title](#)

Mullineaux CW (2014a) Co-existence of photosynthetic and respiratory activities in cyanobacterial thylakoid membranes. Biochim Biophys Acta 1837: 503-511

Pubmed: [Author and Title](#)
CrossRef: [Author and Title](#)
Google Scholar: [Author Only](#) [Title Only](#) [Author and Title](#)

Mullineaux CW (2014b) Electron transport and light-harvesting switches in cyanobacteria. Front Plant Sci 5: 7

Pubmed: [Author and Title](#)
CrossRef: [Author and Title](#)
Google Scholar: [Author Only](#) [Title Only](#) [Author and Title](#)

- Mullineaux CW, Allen JF (1986) The state 2 transition in the cyanobacterium *Synechococcus* 6301 can be driven by respiratory electron flow into the plastoquinone pool. FEBS Lett 205: 155-160**
Pubmed: [Author and Title](#)
CrossRef: [Author and Title](#)
Google Scholar: [Author Only](#) [Title Only](#) [Author and Title](#)
- Mustila H, Paananen P, Battchikova N, Santana-Sanchez A, Muth-Pawlak D, Hagemann M, Aro EM, Allahverdiyeva Y (2016) The Flavodiiron Protein Flv3 functions as a homo-oligomer during stress acclimation and is distinct from the Flv1/Flv3 hetero-oligomer specific to the O₂ photoreduction pathway. Plant and Cell Phys doi: 10.1093/pcp/pcw047**
Pubmed: [Author and Title](#)
CrossRef: [Author and Title](#)
Google Scholar: [Author Only](#) [Title Only](#) [Author and Title](#)
- Nishio JN, Whitmarsh J (1993) Dissipation of the proton gradient in intact chloroplasts. II. The pH gradient monitored by cytochrome f reduction kinetics. Plant Physiol 101: 89-96**
Pubmed: [Author and Title](#)
CrossRef: [Author and Title](#)
Google Scholar: [Author Only](#) [Title Only](#) [Author and Title](#)
- Nomura CT, Persson S, Shen G, Inoue-Sakamoto K, Bryant DA (2006) Characterization of two cytochrome oxidase operons in the marine cyanobacterium *Synechococcus* sp. PCC 7002: inactivation of *ctaD1* affects the PSI:PSII ratio. Photosyn Res 87: 215-228**
Pubmed: [Author and Title](#)
CrossRef: [Author and Title](#)
Google Scholar: [Author Only](#) [Title Only](#) [Author and Title](#)
- Ohkawa H, Pakrasi HB, Ogawa T (2000) Two types of functionally distinct NAD(P)H dehydrogenases in *Synechocystis* sp. strain PCC6803. J. Biol. Chem 275: 31630-31634**
Pubmed: [Author and Title](#)
CrossRef: [Author and Title](#)
Google Scholar: [Author Only](#) [Title Only](#) [Author and Title](#)
- Pils D, Gregor W, Schmetterer G (1997) Evidence for in vivo activity of three distinct respiratory terminal oxidases in the cyanobacterium *Synechocystis* sp. strain PCC6803. FEMS Microbiol 152: 83-88**
Pubmed: [Author and Title](#)
CrossRef: [Author and Title](#)
Google Scholar: [Author Only](#) [Title Only](#) [Author and Title](#)
- Pils D, Schmetterer G (2001) Characterization of three bioenergetically active respiratory terminal oxidases in the cyanobacterium *Synechocystis* sp. strain PCC 6803. FEMS Microbiol Lett 203: 217-22**
Pubmed: [Author and Title](#)
CrossRef: [Author and Title](#)
Google Scholar: [Author Only](#) [Title Only](#) [Author and Title](#)
- Pisareva T, Shumskaya M, Maddalo G, Ilag L, Norling B (2007) Proteomics of *Synechocystis* sp PCC 6803 - Identification of novel integral plasma membrane proteins. FEBS J 274: 791-804.**
Pubmed: [Author and Title](#)
CrossRef: [Author and Title](#)
Google Scholar: [Author Only](#) [Title Only](#) [Author and Title](#)
- Scherer S (1990) Do photosynthetic and respiratory electron transport chains share redox proteins? Trends Biochem Sci 15: 458-62**
Pubmed: [Author and Title](#)
CrossRef: [Author and Title](#)
Google Scholar: [Author Only](#) [Title Only](#) [Author and Title](#)
- Schneider D, Berry S, Rich P, Seidler A, Rögner M (2001) A regulatory role of the PetM subunit in a cyanobacterial cytochrome b₆f complex. J Biol Chem 276:16780-16785**
Pubmed: [Author and Title](#)
CrossRef: [Author and Title](#)
Google Scholar: [Author Only](#) [Title Only](#) [Author and Title](#)
- Schneider D, Berry S, Volkmer T, Seidler A, Rögner M (2004) PetC1 is the major Rieske iron-sulfur protein in the cytochrome b₆f complex of *Synechocystis* sp. PCC 6803. J Biol Chem 279: 39383-39388**
Pubmed: [Author and Title](#)
CrossRef: [Author and Title](#)
Google Scholar: [Author Only](#) [Title Only](#) [Author and Title](#)
- Schultze M, Forberich B, Rexroth S, Dyczmons N, Roegner M, Appel J (2009) Localization of cytochrome b₆f complexes implies an incomplete respiratory chain in cytoplasmic membranes of the cyanobacterium *Synechocystis* sp. PCC 6803. Biochim Biophys Acta 1787: 1479-1485**
Pubmed: [Author and Title](#)
CrossRef: [Author and Title](#)
Google Scholar: [Author Only](#) [Title Only](#) [Author and Title](#)
- Schuermans RM, Schuermans JM, Bekker M, Kromkamp JC, Matthijs HCP, Hellingwerf KJ (2014) The redox potential of the plastoquinone pool of the cyanobacterium *Synechocystis* species strain PCC 6803 is under strict homeostatic control. Plant Physiol 165: 463-475**
Pubmed: [Author and Title](#)
CrossRef: [Author and Title](#)
Google Scholar: [Author Only](#) [Title Only](#) [Author and Title](#)

Shen G, Boussiba S, Vermaas WFJ (1993) Synechocystis sp. PCC 6803 strains lacking photosystem I and phycobilisome function. Plant Cell 5: 1853-1863

Pubmed: [Author and Title](#)

CrossRef: [Author and Title](#)

Google Scholar: [Author Only](#) [Title Only](#) [Author and Title](#)

Suorsa M, Grieco M, Järvi S, Gollan PJ, Kangasjärvi S, Tikkanen M, Aro EM (2013) PGR5 ensures photosynthetic control to safeguard photosystem I under fluctuating light conditions. Plant Signal Behav 8: e22741

Pubmed: [Author and Title](#)

CrossRef: [Author and Title](#)

Google Scholar: [Author Only](#) [Title Only](#) [Author and Title](#)

Trebst A, Harth E, Draber W (1970) on a new inhibitor of photosynthetic electron-transport in isolated chloroplasts. Z Naturforsch 25: 1157-1159

Pubmed: [Author and Title](#)

CrossRef: [Author and Title](#)

Google Scholar: [Author Only](#) [Title Only](#) [Author and Title](#)

Tsunoyama Y, Bernát G, Dyczmons NG, Schneider D, Rögner M (2009) Multiple Rieske proteins enable short- and long-term light adaptation of Synechocystis sp. PCC 6803. J Biol Chem 284: 27875-27883

Pubmed: [Author and Title](#)

CrossRef: [Author and Title](#)

Google Scholar: [Author Only](#) [Title Only](#) [Author and Title](#)

Vass I, Kirilovsky D and Etienne A-L (1999) UV-B radiation- induced donor and acceptor side modifications of Photosystem II in the cyanobacterium Synechocystis sp.PCC 6803. Biochemistry 38: 12786-12794

Pubmed: [Author and Title](#)

CrossRef: [Author and Title](#)

Google Scholar: [Author Only](#) [Title Only](#) [Author and Title](#)

Vermaas W (2001) Photosynthesis and Respiration in Cyanobacteria. eLS.

Pubmed: [Author and Title](#)

CrossRef: [Author and Title](#)

Google Scholar: [Author Only](#) [Title Only](#) [Author and Title](#)

Vicente JB, Gomes CM, Wasserfallen A, Teixeira M (2002) Module fusion in an A-type flavoprotein from the cyanobacterium Synechocystis condenses a multiple-component pathway in a single polypeptide chain. Biochem Biophys Res Commun 294: 82-87

Pubmed: [Author and Title](#)

CrossRef: [Author and Title](#)

Google Scholar: [Author Only](#) [Title Only](#) [Author and Title](#)

Yan J, Kurisu G, Cramer WA (2006) Intraprotein transfer of the quinone analogue inhibitor 2,5-dibromo-3-methyl-6-isopropylbenzoquinone in the cytochrome b6f complex. Proc Natl Acad Sci USA 103: 169-174

Pubmed: [Author and Title](#)

CrossRef: [Author and Title](#)

Google Scholar: [Author Only](#) [Title Only](#) [Author and Title](#)

Yu Q, Feilke K, Krieger-Liszkay A, Beyer P (2014) Functional and molecular characterization of plastid terminal oxidase from rice (Oryza sativa) Biochim Biophys Acta 1837: 1284-1292.

Pubmed: [Author and Title](#)

CrossRef: [Author and Title](#)

Google Scholar: [Author Only](#) [Title Only](#) [Author and Title](#)

Zhang L, Selão TT, Pisareva T, Qian J, Sze SK, Carlberg I, Norling B (2013) Deletion of Synechocystis sp. PCC 6803 leader peptidase LepB1 affects photosynthetic complexes and respiration. Mol Cell Proteomics 12: 1192-1203

Pubmed: [Author and Title](#)

CrossRef: [Author and Title](#)

Google Scholar: [Author Only](#) [Title Only](#) [Author and Title](#)

Zhang P, Allahverdiyeva Y, Eisenhut M, Aro EM (2009) Flavodiiron proteins in oxygenic photosynthetic organisms: Photoprotection of photosystem II by Flv2 and Flv4 in Synechocystis sp. PCC 6803. PLoS ONE 4: e5331

Pubmed: [Author and Title](#)

CrossRef: [Author and Title](#)

Google Scholar: [Author Only](#) [Title Only](#) [Author and Title](#)

MATERIALS AND METHODS

Oxygen Evolution Measurements with a Clark-type oxygen electrode

The effect of different DBMIB concentrations on the net O₂ production was measured with a Clark-type oxygen electrode (Hansatech Ltd, Norfolk, England) at 30°C under 400 μmol photons m⁻² s⁻¹ actinic light applied via a 150 Watt, 21 V, EKE quartz halogen-powered fiber optic illuminator (Fiber-Lite DC-950, Dolan-Jenner, MA, USA). Before measurements the cells were collected and resuspended in fresh growth medium at a chlorophyll concentration of 15 μg mL⁻¹. All the measurements were performed in the presence of 1 mM NaHCO₃.

MATERIALS AND METHODS

Oxygen Evolution Measurements with a Clark-type oxygen electrode

The effect of different DBMIB concentrations on the net O₂ production was measured with a Clark-type oxygen electrode (Hansatech Ltd, Norfolk, England) at 30°C under 400 μmol photons m⁻² s⁻¹ actinic light applied via a 150 Watt, 21 V, EKE quartz halogen-powered fiber optic illuminator (Fiber-Lite DC-950, Dolan-Jenner, MA, USA). Before measurements the cells were collected and resuspended in fresh growth medium at a chlorophyll concentration of 15 μg mL⁻¹. All the measurements were performed in the presence of 1 mM NaHCO₃.

FIGURES

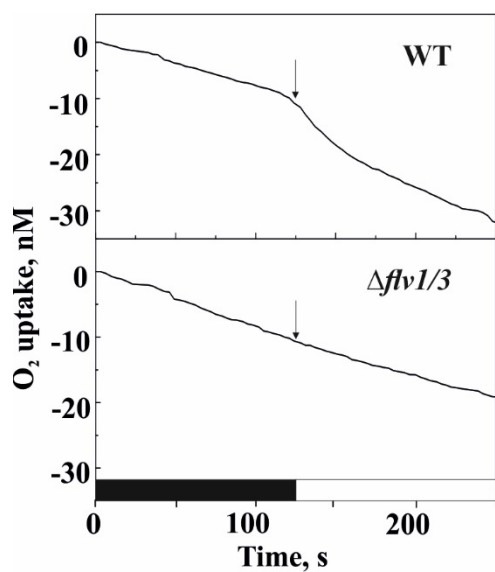


Figure S1. MIMS analysis of O₂ uptake by WT and $\Delta flv1/3$ cells during dark to light transition. Arrows indicate the beginning of illumination with a strong white light at an intensity of $400 \mu\text{mol photons m}^{-2} \text{s}^{-1}$. The slope of the curves does not provide a precise quantitative measure of the rate of O₂ consumption until it is corrected for the isotopic ratio ($^{16}\text{O}/^{18}\text{O}$).

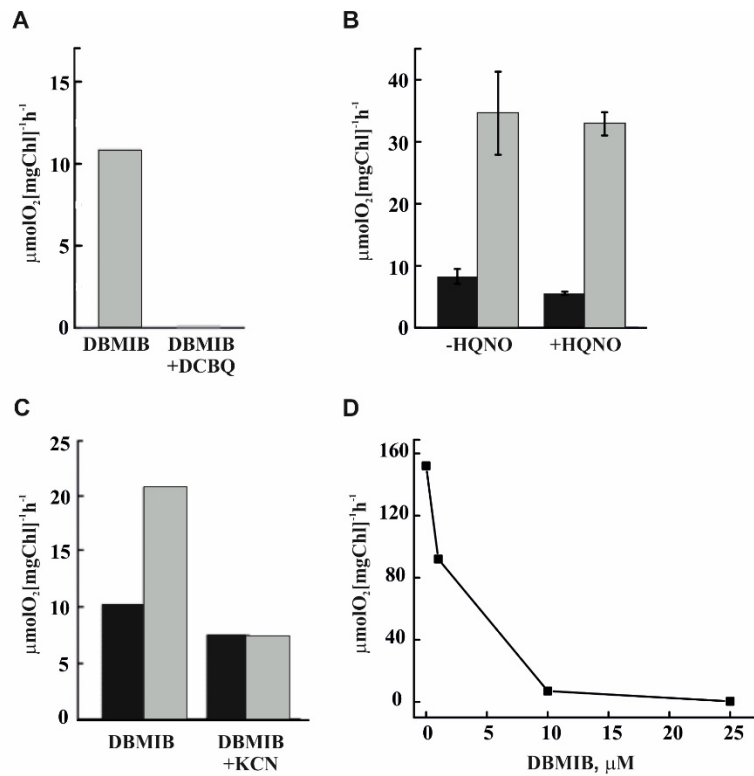


Figure S2. The rates of O_2 uptake and O_2 production in WT *Synechocystis* cells: (A) Light-induced O_2 uptake in the presence of DBMIB and DBMIB+DCBQ; (B) Total O_2 uptake in darkness (black bars) and in the light (grey bars) without and in the presence of HQNO, mean \pm SD, n=3-4; (C) Total O_2 uptake in darkness (black bars) and in the light (grey bars) in the presence of DBMIB or DBMIB+KCN and (D) Net O_2 production in the presence of increasing DBMIB concentrations.

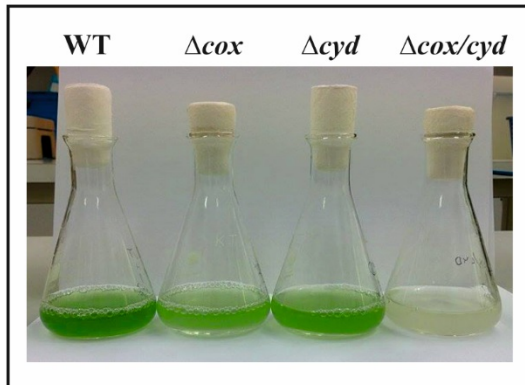
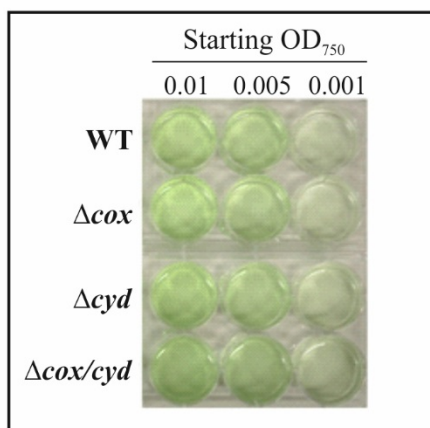
A**B**

Figure S3. The growth of *Synechocystis* WT and RTO-deficient mutant cells under different light conditions: (A) 12 h dark / 12 h high light ($200 \mu\text{mol photons m}^{-2} \text{s}^{-1}$) square cycles for 8 days; (B) constant high light at an intensity of $500 \mu\text{mol photons m}^{-2} \text{s}^{-1}$ for 2 days.

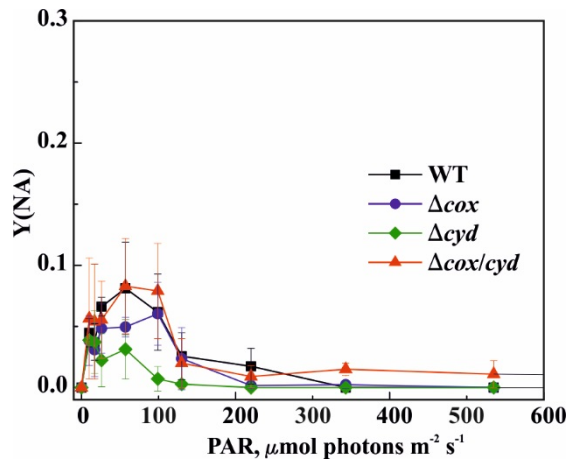


Figure S4. Acceptor side limitation of PS I Y(NA) of the WT and RTO-deficient mutants calculated from the rapid light curves. Mean \pm SD, n=3.

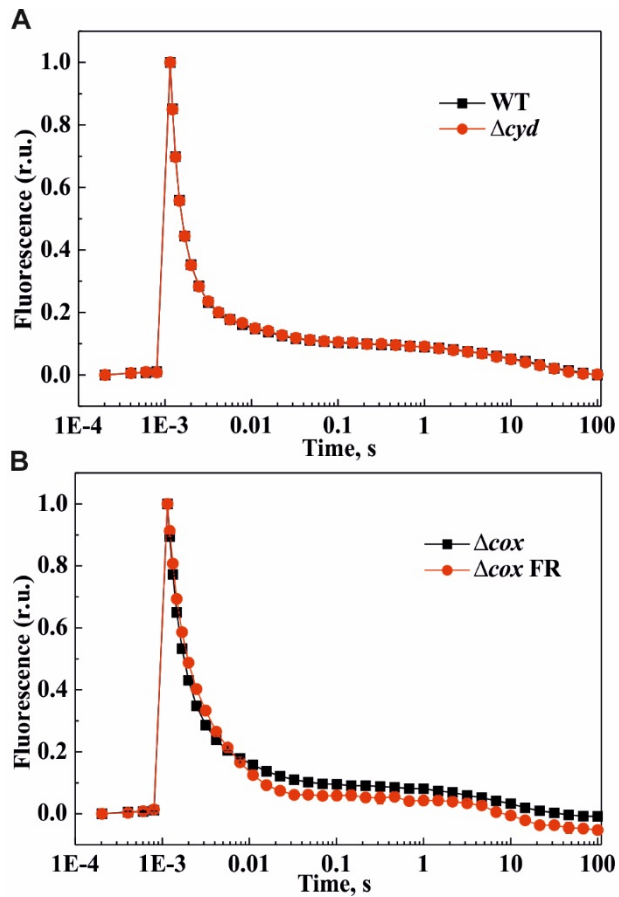


Figure S5. Relaxation of the flash-induced fluorescence yield from WT and RTO mutants: (A) WT and Δcyd cells were dark-adapted for 5 min before the experiment; (B) Δcox cells were dark-adapted for 5 min or pre-illuminated by far-red light before the experiment. Mean \pm SD, n=2-3. Curves were normalized to the same amplitude to facilitate comparison of the kinetics.

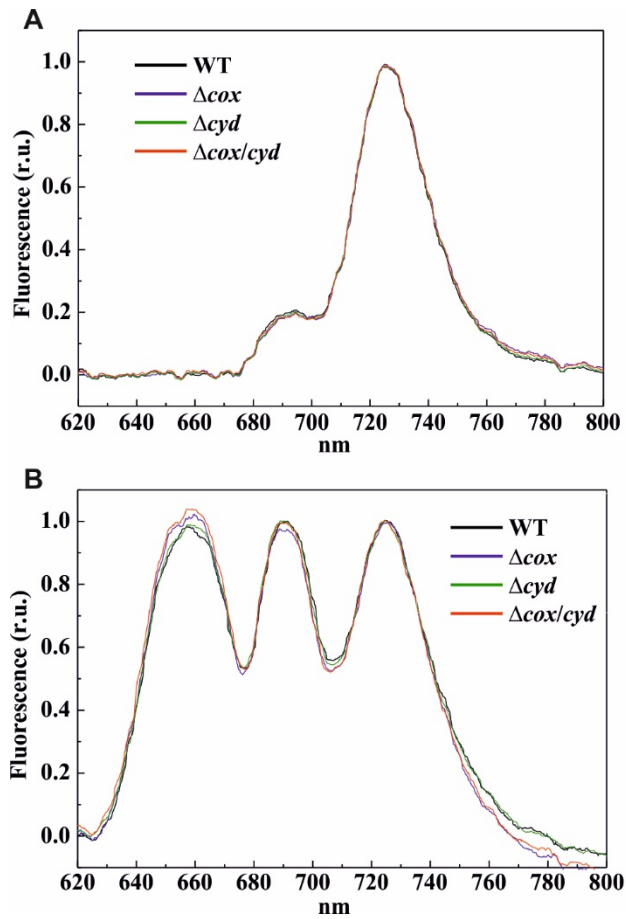


Figure S6. Fluorescence emission spectra recorded at 77K : (A) from the cells excited with 580-nm light; (B) from the cells excited with 440-nm light.

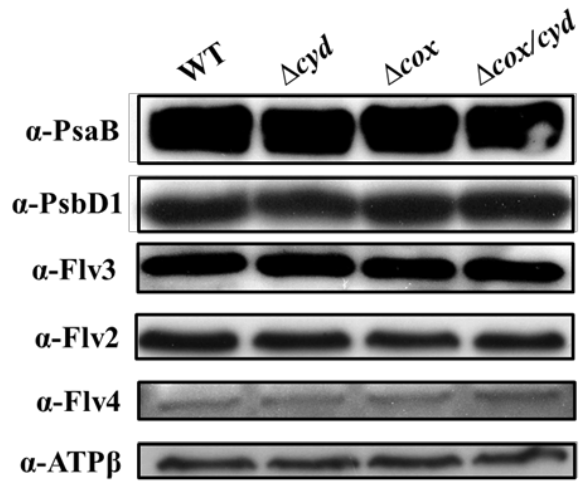


Figure S7. Protein analysis of the WT *Synechocystis* and RTO-deficient mutants.

MATERIALS AND METHODS

Oxygen Evolution Measurements with a Clark-type oxygen electrode

The effect of different DBMIB concentrations on the net O₂ production was measured with a Clark-type oxygen electrode (Hansatech Ltd, Norfolk, England) at 30°C under 400 μmol photons m⁻² s⁻¹ actinic light applied via a 150 Watt, 21 V, EKE quartz halogen-powered fiber optic illuminator (Fiber-Lite DC-950, Dolan-Jenner, MA, USA). Before measurements the cells were collected and resuspended in fresh growth medium at a chlorophyll concentration of 15 μg mL⁻¹. All the measurements were performed in the presence of 1 mM NaHCO₃.